Manganese and iron oxide use at Combe-Grenal (Dordogne, France): A proxy for cultural change in Neanderthal communities

Laure Dayet, Jean-Philippe Faivre, François-Xavier Le Bourdonnec, Emmanuel Discamps, Aurélien Royer, Émilie Claud, Christelle Lahaye, Nadia Cantin, Elise Tartar, Alain Queffelec, et al.

Manganese and iron oxide use at Combe-Grenal (Dordogne, France): A proxy for cultural change in Neanderthal communities

Laure Dayet[a,b], Jean-Philippe Faivre[a], François-Xavier Le Bourdonnec[c], Emmanuel Discamps[b], Aurélien Royer[d], Emilie Claud[a,e], Christelle Lahaye[c], Nadia Cantin[c], Elise Tartar[f], Alain Queffelec[a], Brad Gravina[a], Alain Turq[g], Francesco d'Errico[a,h]

[a]CNRS-Université de Bordeaux, UMR5199 de la Préhistoire à l'Actuel: Culture, Environnement et Anthropologie (PACEA), Université de Bordeaux, Allée Geoffroy Saint Hilaire, CS 50023, F-33615 Pessac Cedex, France

[b]CNRS-Université Toulouse Jean Jaurès,UMR5608 Travaux et Recherches Archéologiquessur les Cultures, les Espaces et les Sociétés (TRACES), Maison de la Recherche, 5, allée Antonio Machado, 31058 Toulouse Cedex 9, France

[c]CNRS-Université Bordeaux Montagne, UMR5060 Institut de Recherche sur les Archéomatériaux – Centre de Recherche Appliqué à l'Archéologie, Maison de l'Archéologie, EsplanadedesAntilles, 33607 Pessac Cedex, France

[d] Biogéosciences, UMR 6282 CNRS, Université Bourgogne Franche-Comté, 6 Boulevard Gabriel, 21000 Dijon, France

[e] INRAP Grand-Sud-Ouest, 140 avenue du Maréchal LECLERC, CS50036, 33323 Begles Cedex 210, France

[f] CNRS-Université Paris I, UMR 7041 Archéologie et Sciences de l'Antiquité (ArScAn), Equipe Ethnologie Préhistorique, Maison de l'Archéologie et de l'Ethnologie, 21 allée de l'Université, 92023 Nanterre cedex, France

[g] Musée Nationale de Préhistoire, Les Eyzies, France

[h] SFF Centre for Early Sapiens Behaviour (SapienCE), University of Bergen, Øysteinsgate 3, Postboks 7805, 5020, Bergen, Norway

Abstract

Neanderthal material culture patterning in Western Europe has been primarily approached from retouched stone tools and associated flake production methods. While considerable effort has been devoted over the past decade to better characterize Middle Palaeolithic lithic techno-complexes (LTCs) in this region, the extent to which they reflect cultural groups still remains unclear. In this respect, integrating other forms of archaeological evidence could provide valuable insights on the cultural significance of late Middle Palaeolithic industrial variability. The site of Combe-Grenal (Dordogne, France) has yielded consistent evidence of mineral pigment use throughout the upper part of the sequence. Here we explore whether mineral pigments might be embedded with an indexical meaning and if changes in pigment exploitation potentially reflect cultural changes. We combined a microscopic use-wear approach with SEM-EDS, pXRF, and XRD analyses of 73 pigment fragments from layers 26 to 11 in order to reconstruct the different stages of their acquisition and use (provenance, selection, processing, function). Our results show manganese oxides to have been used in the lower layers of the Quina LTC, while red and/or yellow iron oxide pieces were employed during the Discoid and Discoid/ Levallois LTCs. This decrease in manganese oxide use correlates with a change in lithic technology and may represent some form of cultural change.

. 1. Introduction

Reliably correlating archaeological assemblage composition with patterns of cultural change remains one of the foremost challenges for Palaeolithic archaeology. This is particularly the case with the late Neanderthal record of Western Europe, where assemblage types are traditionally defined with references to stone tool typology and associated production methods. Consistent efforts over the last decade have made considerable inroads in 'cleaning-up' Middle Palaeolithic industrial taxonomy in a key region of the Neanderthal occupation of Western Europe –south-western France (see Faivre et al., 2017a). By moving away from an emphasis on retouched tool proportions and focusing instead on flake production methods in the form of lithic technocomplexes (LTC), Jaubert (2011, 2014) provided one of the most detailed chrono-cultural syntheses of the Middle Palaeolithic succession in south-western France. This revision highlighted a broad tendency of Levallois-based assemblages to precede those assigned to the Quina flaking system, the latter being overlain by layers in which the Discoid flaking system is dominant. Concentrating on production methods instead of stone tool types avoids pitfalls of typological distinctions, which do not accurately reflect past tool categories (see e.g. Chase and Dibble, 1987). Variations in the proportions of tool types may instead reflect differences in site function (Binford and Binford, 1966; Binford, 1983), raw material constraints, tool resharpening intensity (Dibble, 1984, 1987; Rolland and Dibble, 1990) and the reuse or recycling off lakes and tools (Vaquero, 2011; Turq et al., 2013; Clément, 2014; Gravina and Discamps, 2015).

Considering difficulties in mobilising stone tool typology for identifying consistent cultural groups in the Middle Palaeolithic, recent studies have increasingly turned to technological systems to address potential cultural distinctions (Delagnes and Meignen, 2006). For example, Faivre et al. (2014) demonstrated a clear chronological patterning of the three main Middle Palaeolithic flaking systems - Levallois, Quina, and Discoid -in the deep archaeological sequence of CombeGrenal. A subsequent statistical analysis of well-defined technological data collated from multiple sites in the same region provided a means for better defining Middle Palaeolithic lithic techno-complexes (LTC) in south-western France (Faivre et al., 2017b). This renewed vision of Middle Palaeolithic industrial variability presents a new opportunity to explore how other elements, namely pigment use, can potentially provide additional insights concerning the cultural significance of Neanderthal material culture patterning in this important region of Western Europe. In this respect, the use of manganese and iron oxides during the late Middle Palaeolithic is a well-known but still poorly documented phenomenon of the Neanderthal behavioural repertoire (Demars, 1992; Soressi and d'Errico, 2007; Roebroeks et al., 2012; Bonjean et al., 2015; Heyes et al., 2016; Pitarch Martí and d'Errico, 2018). The site of CombeGrenal has produced one of the rare archaeological sequences from south-western France with evidence for the consistent use of mineral pigments throughout several archaeological layers (Demars, 1992). Here we provide a detailed use-wear, mineralogical and diachronic analysis of mineral pigments from multiple layers comprising CombeGrenal's late Middle Palaeolithic sequence and explore the anthropogenic origin of the pigments, their provenance and possible uses in order to shed new light on the potential cultural meaning of late Middle Palaeolithic LTCs in south-western France.

2. Background

2.1. Mineral pigments in question

Mineral pigments or colouring materials can be defined as geomaterials with the potential for staining other materials. These minerals contain a tinting agent or pigment in the form of iron oxide (e.g. hematite, red), iron oxy-hydroxide (e.g. goethite, yellow), manganese oxide (e.g. pyrolusite, gray to black), manganese oxy-hydroxide (e.g. manganite, black), or mixed oxides (e.g. hollandite, dark gray). Available archaeological evidence suggests that these materials were most often reduced to powder

before use (Couraud, 1988; Watts, 2002; Salomon, 2009; Hodgskiss, 2013). While the most archaeologicallyvisible use of both red and black colouring materials during the Palaeolithic remains parietal art (see e.g. Clottes et al., 1990; Baffier et al., 1999; Chalmin et al., 2003; de Balbín Behrmann and González, 2009; Menu, 2009; Beck et al., 2014), several other uses of these two pigments have equally been documented. Hematite-bearing materials, commonly referred to as 'ochre', are the most common pigments described from archaeological and ethnographic contexts. There potential uses include technical, medicinal, cosmetic, or ritual purposes (Rudner, 1982; Watts, 2002; Rifkin, 2012a), body painting, preserving hides (Audouin and Plisson, 1982; Rifkin, 2011), or as a loading agent in adhesives (Wadley et al., 2004, 2009; Shaham et al., 2010). Potential uses of black manganese oxide, on the other hand, are currently restricted to their direct application to the skin in the form of body painting or drawing (Soressi and d'Errico, 2007; Hodgskiss, 2013) or as an accelerant for igniting fires (Heyes et al., 2016).

Over the last few decades, the exploitation of manganese and iron oxides has been increasingly documented in the Middle Palaeolithic record of Western Europe, demonstrating their widespread use by Neanderthal groups. The most well-documented use of mineral pigments comes from Pech-de-l'Azé I in Dordogne, France (Soressi and d'Errico, 2007). 3D reconstruction of use-wear traces and their comparison with experimental data suggested Neanderthals to have used black manganese fragments to draw on their skin. Since this initial study, several other examples of Middle Palaeolithic red and black oxides have been published, including those from Cueva Anton, Spain (Zilhão et al., 2010); Maastricht, Netherlands (Roebroeks et al., 2012); Ormesson, France (Bodu et al., 2014); and Scladina, Belgium (Bonjean et al., 2015). A recent study of black manganese oxide pieces from both Mousterian (Pech de l'Aze I, Le Moustier, Tabaterie) and Upper Palaeolithic (Laugerie Haute, La Ferrassie, Abri Castanet) sites, which included a geochemical analysis of their composition and a comparison with geological samples, revealed differences in the variability of manganese oxides exploited during the Middle and Upper Palaeolithic (Pitarch Martí and d'Errico, 2018). However, this study did not explore potential differences in mineral pigment exploitation between Middle Palaeolithic lithic techno-complexes. Due to its deep archaeological sequence and setting in a region with a rich record of Middle Palaeolithic occupation, Combe-Grenal is an ideal case study for exploring the distribution and use of black and red/yellow mineral pigments across different late Middle Palaeolithic LTCs.

2.2. The Combe-Grenal sequence: Archaeological background

The rockshelter of Combe-Grenal (Dordogne) lies within a Coniacian limestone escarpment and opens onto a small valley near the Dordogne River (Fig. 1). Since its discovery in 1816, several generations of prehistorians have explored the site's archaeological deposits. Excavations lead by F. Bordes (1955, 1972) from 1953 to 1965 yielded the most important collection of lithic and faunal material from 65 layers attributed to the early and late Middle Palaeolithic. The colouring materials studied here were recovered from layers near the top of this 13 m deep archaeological sequence (layers 26 to 11). Lithic assemblages from these levels have been the subject of multiple typological, technological and techno-economic analyses (Geneste et al., 1997; Turq, 2000a, 2000b; Bourguignon et al., 2004; Faivre, 2011; Faivre et al., 2014, 2017b). The most recent revaluations (Faivre et al., 2014, 2017b) showed many of Bordes' "facies" identified in multiple layers of the site could in fact be grouped together as specific LTC given their similar technological features. In terms of technology, this part of the sequence is characterized by a succession of Quina (layers 26–17), Discoid/Levallois (layers 16; 11–12) and Discoid (layers 13–15) lithic techno-complexes, which depict clear variations in tool typology (Fig. 2).

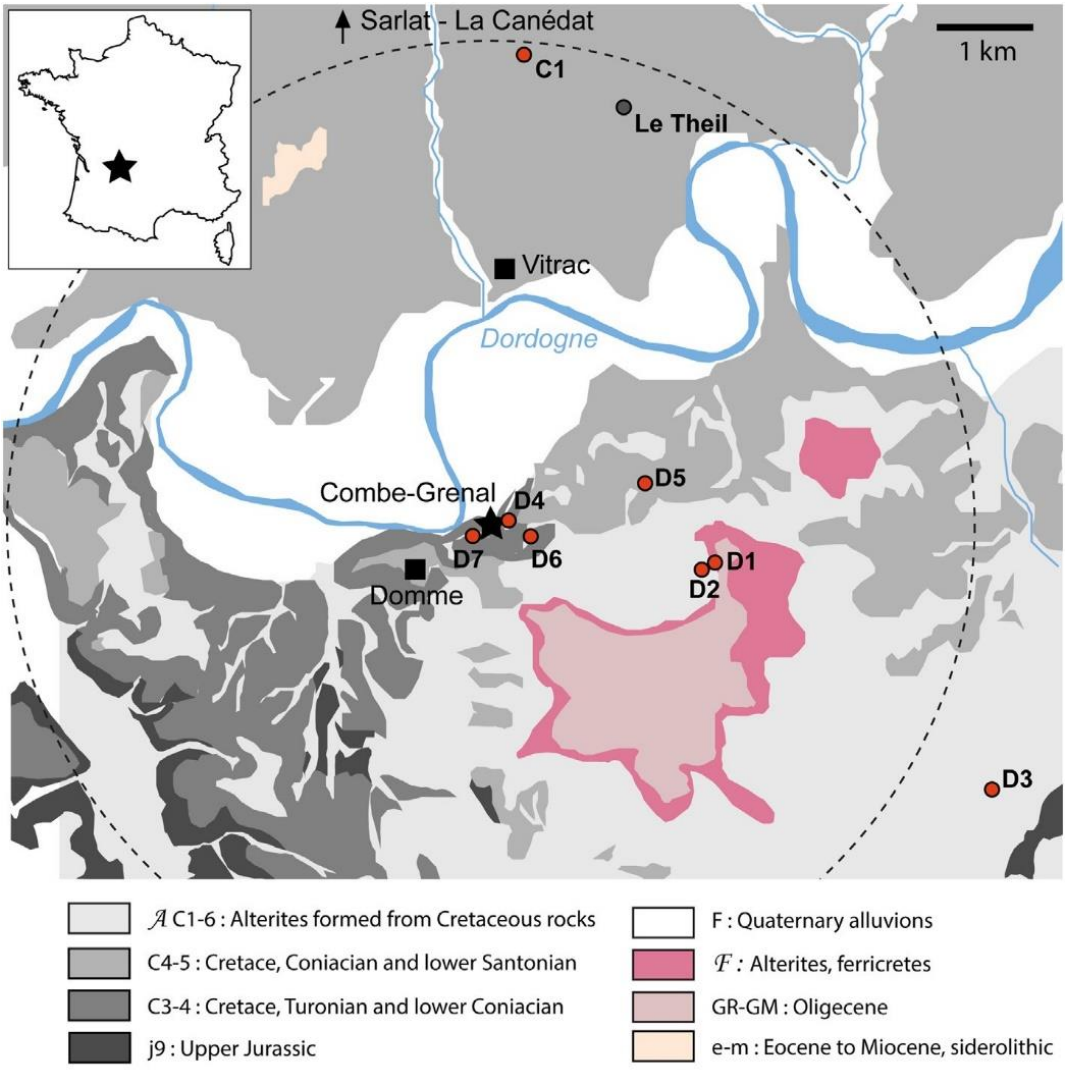

Fig. 1. Location of Combe-Grenal and geology of the region. Red dots indicate the location of some of the iron oxide outcrops identified in the region (listed in Table 2); The black dot indicates the location of the sole local source of manganese reported in the area.

Several use-wear analyses focused on stone tools recovered from the different LTCs (Quina and Discoid/Levallois) during the 80s and 90s (Anderson-Gerfaud, 1981; Beyries, 1987; Beyries and Walter, 1996) produced evidence for wood and hide processing, butchery and, notably, mineral processing. This latter activity was identified on retouched surfaces of several Quina scrapers that also bear red (35 scrapers) and black residues (one scraper), preserved in the distal portion of the retouch scars. A SEM analysis, combined with X-ray elemental characterization, carried out on eight of these tools revealed the presence of hematite, ochre, and manganese oxide residues (Beyries and Walter, 1996). Scrapers were thus interpreted as having very likely been used to process mineral pigments. Recently, one of us (E. Claud) undertook a use-wear analysis of lithics from on-going excavations. Preliminary results for the Discoid/Levallois LTC produced evidence for butchery, and more rarely, scraping bone. No evidence for the processing of minerals or red or black residues that could correspond to colouring materials were identified.

The Middle Palaeolithic occupations of Combe-Grenal are currently beyond the limits of conventional radiocarbon dating. However, several regional syntheses of changes in faunal communities proposed the upper part of the Combe-Grenal sequence to span the period from MIS 5 (130–82 ka) to the beginning of MIS 3 (57–29 ka) (Discamps et al., 2011; Faivre et al., 2014; Discamps and Royer,

2017). Faunal data from on-going excavations has, however, highlighted substantial recovery biases in Bordes' faunal collections (Discamps and Faivre, 2017), calling into question previously proposed chronological models (Guadelli and Laville, 1990; Discamps et al., 2011; Morin et al., 2014). In parallel, an analysis of the small mammal assemblages (Marquet, 1989) highlighted only minimal changes in environmental conditions between the Quina and Discoid/Levallois levels, the former containing several more cold-adapted species, such as snow vole (Chionomysnivalis). Layer 26, however, stands out from the other Quina levels, given the dominance of temperate species that could live in forest conditions. These correlations should, however, be considered with some caution given the limited sample sizes of small mammals from each level.

Layers	Lithic 'phases'	
	Flaking system (LTC)	Dominant typology
11-12	Discoid/Levallois	Denticulates
13-15	Discoid	
16	Discoid/Levallois bladelet	
17-19	Quina	Denticulates/ Scrapers (III)
20		Denticulates (II)
21-26		Scrapers (I)

Fig. 2. Top of the Combe-Grenal sequence with typological and technological attributions of each of Bordes' layers (modified after Faivre et al., 2014).

3. Material and methods

3.1 Material

3.1.1 Archaeological collection

In the F. Bordes collections of Combe-Grenal, staining mineral-rich rocks, such as iron and manganese oxides, recovered by Bordes from Combe-Grenal were found partially sorted in separate boxes from the lithic material when we began our study. While this material had been partially inventoried by P.-Y. Demars (1992), we conducted a careful examination of the unsorted material in order to identify any additional fragments of iron and manganese oxides. Sorting was limited to the site's late Middle Palaeolithic layers (layers 26–11), which had previously been shown to contain the highest frequency of staining minerals (Demars, 1992). The main types of mineral pigments identified in our study are presented in Fig. 3, and descriptions of all archaeological samples are available in Table 1 and Table SI 1.

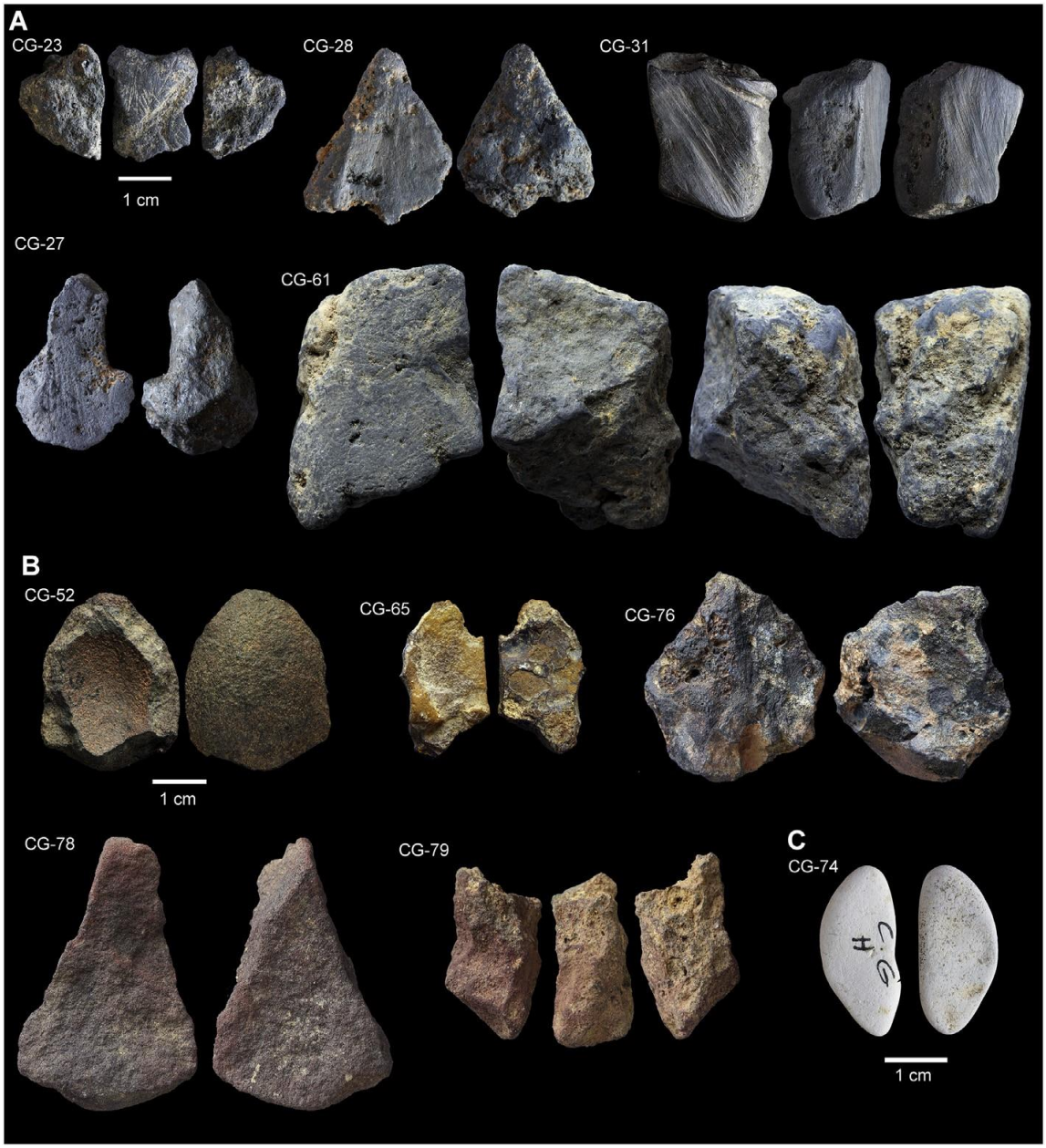

Fig. 3. Sample of archaeological black (A), red, yellow (B) and white (C) pigment fragments studied.

Archaeological information				Macroscopic examination						
N°	Layer	LTC[a]	Lithic typology	Colour	Length (cm)	Width (cm)	Thick. (cm)	Mass (g)	Type of blank	Type of oxide
CG-16	K (22)	Quina	Scrapers	Black	5.3	4.3	2.2	95.7	Raw nodule	Mn oxides
CG-17	K (22)	Quina	Scrapers	Gray/anthracite	2.3	2.0	1.4	8	Fragment	Mn oxides
CG-18	N (25)	Quina	Scrapers	Anthracite	3.6	2.2	1.1	11.8	Fragment	Mn oxides
CG-19	N (25)	Quina	Scrapers	Anthracite	3.3	1.8	0.9	6.3	Fragment	Mn oxides
CG-20	N (25)	Quina	Scrapers	Gray	2.2	2.0	0.7	4.1	Fragment	Mn oxides
CG-21	N (25)	Quina	Scrapers	Black/anthracite	6.5	22	21.9	13.8	Fragment	Mn-Co oxides
CG-22	N (25)	Quina	Scrapers	Black/anthracite	2	0.7	0.8	0.8	Worked fragment	Mn oxides
CG-23	N (25)	Quina	Scrapers	Black/anthracite	2	1.5	1.4	5.2	Worked fragment	Mn oxides
CG-24	N1 (26)	Quina	Scrapers	Gray	4.5	2.0	1.3	18.5	Worked nodule	Mn oxides
CG-25	M (24)	Quina	Scrapers	Anthracite	1.8	1.3	1.0	4	Worked fragment	Mn oxides
CG-26	N (25)	Quina	Scrapers	Gray	2.1	2.0	1.5	8	Worked fragment	Mn oxides
CG-27	N (25)	Quina	Scrapers	Gray	3.2	2.1	1.2	10.4	Worked fragment	Mn oxides
CG-28	M (24)	Quina	Scrapers	Black/anthracite	3.1	2.1	1.2	9	Worked fragment	Mn oxides + Fe oxides
CG-29	M (24)	Quina	Scrapers	Anthracite/gray	3.1	1.3	0.8	3.5	Flake	Mn oxides
CG-30	M (24)	Quina	Scrapers	Black/gray	3	1.8	1.5	11.1	Worked fragment	Mn oxides
CG-31	M (24)	Quina	Scrapers	Black/anthracite	3	2.4	1.3	14.5	Worked fragment	Mn oxides
CG-32	M (24)	Quina	Scrapers	Black/anthracite	2.3	1.3	1.1	5.1	Fragment	Mn oxides
CG-33	L (23)	Quina	Scrapers	Black/anthracite	1.5	1.1	0.7	1.8	Fragment	Mn oxides
CG-34	L (23)	Quina	Scrapers	Black/anthracite	1.3	0.6	0.4	0.6	Fragment	Mn oxides
CG-35	L (23)	Quina	Scrapers	Black/anthracite	1.2	0.8	0.6	1	Fragment	Mn oxides
CG-36	L (23)	Quina	Scrapers	Anthracite/brown yellow	2.3	1.4	1.2	4.4	Worked fragment	Mn oxides + Fe oxides
CG-37	L (23)	Quina	Scrapers	Gray/brown yellow	2.1	1.5	1.1	3.7	Fragment	Mn oxides
CG-38	L (23)	Quina	Scrapers	Black/anthracite	2.4	2.0	1.1	7.2	Worked fragment	Mn oxides
CG-39	L (23)	Quina	Scrapers	Anthracite/gray	2.3	1.4	1.0	5.3	Worked fragment	Mn oxides
CG-40	L (23)	Quina	Scrapers	Anthracite/dark green	4.4	3.9	0.8	17.9	Cortical flake	Mn oxides
CG-41	L (23)	Quina	Scrapers	Anthracite	2.7	1.7	1.0	8.7	Worked fragment	Mn oxides
CG-42	L (23)	Quina	Scrapers	Anthracite	2.1	1.6	0.8	3	Fragment	Mn oxides
CG-43	L (23)	Quina	Scrapers	Anthracite	1.9	1.6	0.9	4	Worked fragment	Mn oxides
CG-44	L (23)	Quina	Scrapers	Anthracite gray	3.9	2.6	2.1	29.9	Worked fragment	Mn oxides
CG-45	L (23)	Quina	Scrapers	Anthracite gray	1.9	1.5	0.7	1.6	Fragment	Mn oxides
CG-46	L (23)	Quina	Scrapers	Anthracite gray	1.6	1.6	0.8	3.4	Fragment	Mn oxides
CG-47	L (23)	Quina	Scrapers	Anthracite gray	1.7	1.5	0.9	2.6	Fragment	Mn oxides
CG-48	L (23)	Quina	Scrapers	?	1.8	1.4	0.6	2.3	Worked fragment	Mn oxides
CG-49	L (23)	Quina	Scrapers	Anthracite	2	1.6	0.8	3.7	Fragment	Mn oxides
CG-50	L (23)	Quina	Scrapers	Gray/dark brown	2.2	2.0	1.9	10.5	Fragment	Mn oxides
CG-51	L (23)	Quina	Scrapers	Dark brown, dark red	3.3	2.5	1.1	12.2	Fragment	Fe oxides + Mn oxides
CG-52	L (23)	Quina	Scrapers	Black, dark red	2.3	1.8	0.8	6.2	Fragment	Fe oxides
CG-53	L (23)	Quina	Scrapers	White	2.2	1.8	0.6	2.1	?	Calcite, chalk
CG-54	L (23)	Quina	Scrapers	White	2.5	1.6	1.1	3.5	?	Calcite, chalk
CG-55	L (23)	Quina	Scrapers	White	1.6	1.5	0.8	2	?	Calcite, chalk
CG-56	K (22)	Quina	Scrapers	Anthracite/gray	1.3	1.2	1.0	3	Worked fragment	Mn oxides
CG-57	K (22)	Quina	Scrapers	Black	2.5	2.2	1.5	9.6	Worked fragment	Mn oxides
CG-58	K (22)	Quina	Scrapers	Black	2.4	2.1	0.7	7.9	Worked fragment	Mn oxides
CG-59	K1 (21)	Quina	Scrapers	Gray	1.8	1.1	0.6	2	Worked fragment	Mn oxides
CG-60	K (22)	Quina	Scrapers	Ocre, rouge, jaune	8.2	7.7	5.6	400.1	?	Fe oxides
CG-61	J (18)	Quina	Denticulates/scrapers	Antracite/brown	3.4	4.0	2.7	61.3	Worked fragment	Mn oxides
CG-62	I (17)	Quina	Denticulates/scrapers	Dark red purple, light brown	1.5	1.3	0.4	1.3	?	Fe oxides
CG-63	I (17)	Quina	Denticulates/scrapers	Anthracite/gray	1.5	1.3	0.8	2.8	?	Mn oxides
CG-64	I (17)	Quina	Denticulates/scrapers	Dark red	5.2	4.1	0.8	25.1	Raw nodule	Fe oxides
CG-65	I (17)	Quina	Denticulates/scrapers	Yellow, brown	2.9	1.6	0.7	2.5	?	Fe oxides
CG-66	H2 (16)	Lev./Disc. Bladelet	Denticulates	Anthracite/gray	4.3	3.7	2.0	50.7	Fragment	Mn oxides
CG-67	H (15)	Discoid	Denticulates	Anthracite/brown yellow	2	1.3	0.8	3.2	?	Mn oxides
CG-68	H (15)	Discoid	Denticulates	Dark red/dark yellow	3.8	3.3	3.1	53.4	Fragment	Fe oxides
CG-69	H (15)	Discoid	Denticulates	Dark red/dark yellow	2.6	2.1	1.3	6.7	Fragment	Fe oxides
CG-70	H (15)	Discoid	Denticulates	Dark red/black/dark yellow	1.8	1.8	0.9	3.2	Fragment	Fe oxides
CG-71	H (15)	Discoid	Denticulates	Dark red/dark yellow	1.7	1.2	0.4	0.9	?	Fe oxides
CG-72	H (15)	Discoid	Denticulates	Dark red/dark yellow	2.1	1.3	1.2	3.5	Fragment	Fe oxides
CG-73	H (15)	Discoid	Denticulates	Dark red/black/dark yellow	1.8	1.2	0.6	1.4	Flake?	Fe oxides
CG-74	H (15)	Discoid	Denticulates	White	2.7	1.2	0.8	3.1	?	Calcite, chalk
CG-75	G (14)	Discoid	Denticulates	Dark red/black/dark yellow	6	5.3	3.6	91.6	Fragment	Fe oxides
CG-76	G (14)	Discoid	Denticulates	Dark red/black	3.5	3.2	2.2	19.2	Fragment	Fe oxides
CG-77	G (14)	Discoid	Denticulates	Dark red/black	2.8	2.3	1.3	8.9	Fragment	Fe oxides
CG-78	G (14)	Discoid	Denticulates	Dark red/red	4.7	3.0	1.8	12.9	Flake/fragment	Fe oxides
CG-79	G (14)	Discoid	Denticulates	Red	2.9	1.5	1.3	6.6	Fragment	Fe oxides
CG-80	G (14)	Discoid	Denticulates	Red	3.2	1.4	0.9	3.9	Fragment	Fe oxides
CG-81	G (14)	Discoid	Denticulates	Light pink, dark red	2.1	2.2	1.4	6.3	?	Fe oxides
CG-82	E2 (12)	Discoid/levallois	Denticulates	Dark red/black/dark yellow	7.5	5.4	4.3	169.9	Fragment	Fe oxides
CG-83	E2 (12)	Discoid/levallois	Denticulates	Dark red/dark yellow	3	3.0	2.2	19.5	Fragment	Fe oxides
CG-84	E2 (12)	Discoid/levallois	Denticulates	Light brown, anthracite/dark brown	4.2	2.9	2.6	28.6	?	Fe oxides
CG-85	E2 (12)	Discoid/levallois	Denticulates	Light pink, dark red	2.4	1.7	1.6	6.3	?	Fe oxides
CG-86	E1 (11)	Discoid/levallois	Denticulates	Anthracite/dark brown	3.5	2.0	1.6	17.8	Fragment	Mn oxides
CG-87	E1 (11)	Discoid/levallois	Denticulates	Dark red/black	2.8	2.6	1.6	17.7	Fragment	Fe oxides
CG-88	E1 (11)	Discoid/levallois	Denticulates	Light pink, dark red	1.7	1.3	1.3	3	Fragment	Fe oxides

[a] Lithic technocomplex.

Table 1 General description of the mineral pigment fragments from the upper part of the Combe-Grenal sequence

3.1.2 Geological reference collection

Potential iron oxide sources were surveyed within an approximately analysis of the small mammal assemblages (Marquet, 1989) highlighted 5 km radius of the site (Fig. 1). Several sources of ferruginous rocks are located within a few hundred metres to a few kilometres of the site and exist primarily as eroded in situ veins and crusts developed within Upper Cretaceous limestones (D1, D2, D3, D4) or pedogenic nodules (D5, D6, D7) formed from these crusts (Table 2) (Astruc, 1990). Apart from a vein in unaltered limestone (D4), all of the closest outcrops are found within a deep sequence of alterites that formed in lacustrine conditions during the Oligocene. Ferruginous nodules are found in multiple locations within a few hundred metres from the site, with the only in situ alterites containing concretions and nodules located < 1 km to the south east. Nodules are also found at the top of Cretaceous formations (C1) to the north of the site. Although a 'siderolithic' facies had previously been described (Capdeville and Rigaud, 1987), we were unable to find nodules where this facies is reported on 1/50000 geological maps.

A recent review of manganese oxide outcrops in the Dordogne identified only one source (Le Theil near La Canéda) within a 5 km radius around Combe-Grenal, with the next closest sources near Sarlat, around 10 km from the site. As data was already available for these sources (Pitarch Martí and d'Errico, 2018), they were not resampled during our work.

Outcrop code	Town	Lieu-dit'	Location of the occurrences	Latitude	Longitude	Geological description	Formation
D1	Domme	Jacoumard	Astragale along a road	N44°48′10″	E1°15′15.5″	Concretions within alteritic sands	Alterites
D2		Jacoumard	Astragale along a road	N44°48′26″	E1°15′04″	Concretions and nodules within brown soil	Alterites
D3		Liaubou bas	Sand quarry	N44°47′02.5″	E1°17′31.5″	Concretions and veins within alteritic sands	Alterites
D4		Combe-Grenal	Section along a road	N44°48′23″	E1°13′34.5″	Veins within fresh limestone	Coniacian
D5		Giverzac	Covering the soil	N44°48′38″	E1°14′42″	Nodules within a brown soil	Pedogenic
D6		Combe-Grenal	Astragale along a stream	N44°48′22″	E1°13′48″	Nodules within a brown soil	Pedogenic
D7		Combe-Grenal	Astagale along a stream	N44°48′22″	E1°13′29.5″	Nodules within a brown soil	Pedogenic
C1	La Canéda	Curboursil	Covering the soil	N44°51′02″	E1°13′41″	Nodules within a brown soil	Pedogenic
Huy	Huy (Belgium)		Section along a road			Oolithic hematite	Lower famenian

Table 2 Description and location of iron oxide sources sampled in this study.

3.2. Methods

All archaeological pieces were submitted to a technological, usewear (stereomicroscope), chemical (SEM-EDS, pXRF) and structural analyses (XRD). The first two focused on characterising traces of human modification, while the latter two characterized their elemental and mineral composition. All artefacts were analyzed using non-destructive and non-invasive methods.

3.2.1. Macroscopic examination

All archaeological pigments were examined with a Leica S8 APO stereomicroscope to characterize raw material types and identify traces of anthropogenic modification. Material was photographed with a motorized Leica Z6 APOA equipped with a DFC420 digital camera linked to LAS Montage and Leica Map DCM 3D software packages. Hue, size, weight, texture (i.e. clay to silt: fine-grained; sand: coarsegrained), structure (granular, massive, laminated), degree of porosity, presence of cortex or patina, identifiable mineral particles and fossils were systematically recorded. The identification of human modifications was based on criteria available in Salomon (2009), Hodgskiss (2010), Rifkin (2012b), and Dayet et al. (2013). We also recorded evidence of intentional fracturation and crushing (points of impact,

flake scars, negative and positive bulbs), as well as surface features (number, location, and section of the facets, orientation and type of striation) referable to rubbing, grinding or scraping.

3.2.2. Chemical and mineralogical analyses

Of the 73 mineral-rich fragments identified from the site, 39 were selected for portable energy dispersive X-ray fluorescence spectrometry (pXRF), 31 for scanning electron microscopy coupled with energy dispersive spectrometry (SEM-EDS), and 16 for X-ray diffraction (XRD). This sample reflects the variability of colour, texture and structure in the assemblage. Analyses systematically concerned the flatter surface of the archaeological pieces with the minimum of post-depositional crusts (see Dayet et al., 2013, 2014 for more details concerning the analytical protocol). All fragments were cleaned with an alcoholic solution prior to analysis.

The elemental and mineral composition of the archaeological samples was determined by SEM-EDS and XRD analyses. A JEOL 6460 LV SEM instrument equipped with a low vacuum system was used for imagery and analysis without any specific preparation (coating) of the sample. Semi-quantitative analyses were carried out directly on the surface of complete archaeological pieces using an EDXS Oxford XMax 20 spectrometer coupled to the SEM instrument. All objects were observed under similar magnification (×100, ×200; ×1000, ×2000, and sometimes as high as ×5000). The distribution, size, and shape of minerals measuring > 1 µm were recorded, and data are presented as mass weight % of oxide (stoichiometric conversion). Structural phases were determined by X-ray diffraction using a Bruker D8 Advance diffractometer with the Bragg-Brentano geometry and equipped with a PSD Lynxeye detector operating with a Cu Kα radiation (λ = 1.5405 Å). A divergent slit of 0.2 mm was used in order to limit the divergence of the incident rays. Mineral phases were identified based on data available in the ICDD database (PDF2).

In order to compare data from archaeological iron oxides with the geological reference collection, we used portable XRF (pXRF) measurements, as they are both quicker and record more trace elements than elemental analyses performed with an SEM-EDS. Prior to analysis, the 31 geological samples were fractured with a hammer. Multiple XRF measurements were obtained from these fresh fractures, in order to take into account the heterogeneity of the material. The pXRF measurements were carried out using an Ametek portable SPECTRO xSORT X-ray fluorescence spectrometer equipped with a silicon drift detector (SDD) and an excitation source of 40 kV, 0.1 mA. Measurements were acquired in the air (no detection of Na, Mg, Al) with a constant working distance by fixing the spectrometer to a lead receptacle. A12 mm^2area was analysed using spectra acquisition times of 120 s. The spectrometer's internal consistency was assured using an automated measure of the contents of the machine's metal shutter. A CRM-683 standard was also used to ensure the reproducibility of the measurements. For ferruginous rocks, an empirical calibration was used based on the Lucas-Tooth and Price methodology (Lucas-Tooth and Price, 1961). This calibration method was improved from previous studies (see Dayet et al., 2014; Queffelec et al., 2017) by increasing the acquisition time (120 s), preparing pellets (< 80 µm grain-size powder mixed with 3% of wax), and selecting homemade standards where more trace elements are dosed (six laboratory specific, five international references). “Theoretical” and “measured” data was compared in absolute weight oxide percentages. A good adequacy between the two was achieved for Si, Fe, Mn, Ca, K, Ti, As, Rb, V and Sr (R^2 = 1.0; y = 1.0; Fig. SI 1). No similar empirical calibration was done for manganese oxides due to higher methodological constraints (the presence of Ba as a minor element) and the relevance of the results obtained from the SEM-EDS analyses. Data are presented as mass weight % of oxide (stochiometric conversion).

3.2.3. Data treatment

Elemental and mineralogical data were used to: 1) distinguish iron from manganese oxides; 2) identify potential selection criteria; and 3) discuss provenance. Pieces were attributed to either manganese or iron oxides only when oxide concentration exceeded 10%. Each group was treated

separately. For manganese oxides, a hierarchical clustering (Ward method) followed by a principal component analysis (PCA) was conducted on the semi-quantitative SEM-EDS data by using the centred log ratio (clr) (Aitchison, 1986). Using clr values smoothes differences between major and trace elements. The following elements, expressed as weight % of oxide, were taken into account: Al_2O_3, SiO_2, MnO_2, Fe_2O_3 and BaO. Other elements were excluded when they displayed more than one third of missing values or showed a heterogeneous distribution likely due to their presence in sediments adhering to the surface of objects (P, K, Ca). Although often absent, Ba was included in our study, as this element appears as a minor and sometimes a major element in several samples. A similar approach was followed for iron oxide pieces (i.e. a hierarchical clustering followed by a PCA of the SEM-EDS clr transformed data) and exclusion of elements with a third of missing values. We nevertheless included Mn as it appears as a minor element in several samples. Elements susceptible to deriving from sediment deposits were not removed in this case, as SEM observation showed they represent an integral component of the samples. Eight elements were retained for the statistical analysis of iron oxides: Al_2O_3, SiO_2, P_2O_5, K_2O, CaO, MnO_2, Fe_2O_3.

In order to compare archaeological iron oxides with our geological reference samples, we carried out a PCA of pXRF values. Only the geological pieces are taken into account in this analysis, the archaeological measurements are plotted for comparative purposes. The same selection criteria for retaining elements for the statistical treatment of archaeological pieces were applied to the selection of elements used to characterize reference collections. The following elements were chosen: SiO_2, Fe_2O_3, MnO, CaO, K_2O, TiO_2, V_2O_5, As_2O_3. Both centred log ratios and log values weighted by Fe_2O_3 concentration (alr) were employed. The latter transformation has been frequently and successfully used to explore the provenance of iron oxides (see for example Popelka-Filcoff et al., 2007; Dayet et al., 2016; MacDonald et al., 2018).

In all statistical treatments, missing values were replaced by the detection limit multiplied by 0.6. All statistical analyses and data treatments were carried out with CODAPAK 2.0 (Comas-Cufí and ThióHenestrosa, 2011) and JMP® software packages (Version 13.SAS Institute Inc., Cary, NC, 2016).

The frequency per layer and mineralogical composition of mineral pigments were submitted to a Fisher's exact test to establish to what extent their occurrence should be attributed to chance (null hypothesis). We performed a simulation of this test with random resampling and calculated the probability that the null hypothesis is valid after a million randomizations.

4. Results

Our sorting of Combe-Grenal archaeological material produced an additional 33 mineral fragments for an overall assemblage comprising 73 pieces that feature red, gray, black, and, more rarely, brown and yellow shades (Fig. 3). Several pieces produce a coloured streak or stain when in contact with a plastic bag or fingers. In other cases, their colour and the absence of flake scars distinguishes them from knapped siliceous and volcanic rocks. We also identified and analysed several white fragments with a high staining power (Fig. 3). Among the selected 73 pieces of mineral pigments, 44 were classified as black, 25 as yellow or red, and 4 as white pigments. This classification is based on colour, composition when chemical analyses were performed, and colour of the streak when the pieces produced one. Despite their colour, two black and dark brown pieces do not contain manganese oxides. These pieces instead consist of massive, crystalline iron oxy-hydroxides forms and were included in the group of yellow and red mineral pigments. When ground or scraped, they would produce brown yellow (goethite-rich) or dark red (hematite-rich) powder instead of the gray to black powder generally produced by manganese oxides. Results of the elemental and mineralogical characterization are reported in Table 3.

Sample	Layer	Petrology		Elemental composition SEM		Mineralogy DRX	
		Rock texture	Rock fabric	Mn/Fe phases[a]	Other phases[a]	Mn or Fe phases	Other minerals
Manganese oxides							
CG17	22	Clay-sand	Massive, crystalline	**Mn**-(Si) + **Mn**-Ba	Si, Al, K (Fe)	–	–
CG21	25	Clay-silt	Granular	**Mn**-Al-(Co)	Al, Si, Fe, K	Lithiophorite (manganosite)	**Quartz** (bohmite?)
CG23	25	Sand	Massive	**Mn**-(Fe, Al, Si)	Si, Al	–	–
CG26	25	Clay-sand	Massive, crystalline	**Mn** + **Mn**-Ba	Si	**Pyrolusite** (Ramsdellite?)	(Quartz)
CG27	25	Clay-sand	Massive, crystalline	**Mn**-Ba + **Mn**	(Al)	**Pyrolusite** (Ramsdellite?)	–
CG28	24	Clay-silt	Granular	**Mn**-Fe-(Si, Al) + **Fe**-Mn-(Si, Al)	Si	**Pyrolusite**, Goethite, manganite (Birnessite/kaolinite group)	Quartz
CG30	24	Sand	Massive	**Mn**-(Fe, Al, Si)	Si	–	–
CG31	24	Sand	Massive	**Mn**-(Si, Al, Fe, Ba)	Si, Al, Fe	**Pyrolusite**, Ramsdellite, Birnessite/koalinite group	(Quartz?)
CG36	23	Sand	Massive	**Mn**-Fe		**Pyrolusite**, Goethite	(Quartz)
CG40	23	Clay-silt	Granular	**Mn**-(Fe)	Si, Al	–	–
CG41	23	Sand	Massive	**Mn** + **Mn**-Ba	Si, Al (Fe, K, Ba)	**Pyrolusite**	(Quartz)
CG47	23	Clay-silt	Finely granular	Mn-Si-Al-(Ba, Fe) + **Mn**-Ba + **Mn**-Fe	Si, Fe, Al	–	–
CG48	23	Sand	Massive	**Mn**-Ba-(Si, Al)	Si, Al, Fe (Mg, Ti)	–	–
CG49	23	Sand	Massive, granular cortex	**Mn** + Mn-Mg-Si	Si, Al (Fe, Ca, K)	**Pyrolusite**	(Quartz)
CG58	22	Sand	Lightly laminated	**Mn**-(Si)	Ca, P, Si (Al)	Pyrolusite, Manganite (Birnessite/kaolinite group)	**Quartz**, **h**ydroxylapatite
CG59	21	Clay-sand	Massive, crystalline	**Mn**	Si, Al, Ca, Fe, (P, K)	–	–
CG67	15	Sand	Massive	**Mn**	Ca, Si, Al (Fe, K)	–	–
CG84	12	Clay-sand	Massive, mixed	**Mn**-Ba	Ca, Si, Al (Fe)	–	–
CG86	11	Clay-sand	Granular, massive	**Mn**	Ca, Si, Al (P, K)	Pyrolusite (manganite?)	**Calcite**, quartz
Iron oxides							
CG52	23	Clay-silt	Botryoïdal	**Fe**-(Si, Al)	Si,Al (K)	**Goethite**	Quartz, calcite
CG65	17	Sand	Lightly laminated	**Fe**-(Si, Al)	Ca, Si, Al, Fe (K)	Goethite	**Calcite**, quartz (clay mineral?)
CG69	15	Clay-silt	Granular	**Fe**-Si-(Al)	Si, Al, Fe, Ca (K, Mn)	**Goethite**	Quartz
CG70	15	Sand	Massive, concentric lamination	**Fe**-(Si, Al)	Si, Al, Fe, Ca	–	–
CG76	14	Sand	Massive	**Fe**-(Si, Al)	Si, Al, Fe, Ca (P)	–	–
CG77	14	Clay-silt	Granular, laminated	**Fe**-(Si, Al)	Si, Fe, Al (K, Ca)	**Hematite**	Quartz
CG78	14	Clay-silt	Granular	**Fe**-Si-(Al)	Si (Fe, Al)	–	–
CG79	14	Clay-silt	Massive	**Fe**-(Si, Al)	Si, Ca, Fe (Al, K)	**Hematite**, **Goethite**	Quartz, calcite
CG81	14	Clay-sand	Massive, granular	**Fe**-(Si, Al) + **Fe**-Mn	Si, Al, Fe	–	–
CG83	12	Clay-sand	Massive, concentric lamination	**Fe**-(Si, Al) + Fe-(Mn)	Si, Al, Fe (K, Ti)	–	–
CG85	12	Clay-sand	Massive, granular	**Fe**-Si-(Al)	Ca, Si, Al (K)	–	–
CG87	11	Sand	Massive	**Fe**-(Si, Al)	Si, Ca (Al, K)	**Goethite**	Quartz (chlorite? Calcite?)
White piece							
CG74	15	Clay	Massive	Ca		–	–

[a] In bold: main element.
[a] In brackets: minor element.

Table 3 Elemental and mineralogical composition of the Combe-Grenal archaeological pieces analysed by SEM-EDS and XRD.

4.1. Black mineral pigments

4.1.1. Raw material composition

This group comprises 44 gray to black pieces that contain manganese oxides or oxy-hydroxides and produce a dark streak when rubbed. Their composition is summarized in Table 3 and detailed results are presented in Tables SI 2 and 3 (19 pieces analysed). Most black pieces are composed of almost pure pyrolusite (βMnO_2), in association with traces of manganite ($\gamma MnO(OH)$), ramsdellite (βMnO_2) and possibly birnessite ($(Ca,Na,K)_x(Mn^{4+},Mn^{3+})_6O_{12}$). Although not detected by XRD, mixed oxides containing barium were identified by SEM-EDS analyses (Table 3; Table SI 2) and could represent romanechite, hollandite or some kind of poorly-crystallized Mn-Ba phases. One of the analysed pieces (CG21) contains a Mn-Co oxide, a variation of lithiophorite, (Co,Mn)O(OH), with probable atomic replacement of Al in the structure (bohmite AlO(OH) structure). Manganese oxides are associated with iron oxy-hydroxide goethite ($\alpha FeO(OH)$) in two pieces (CG28 and CG36). Iron is present as a minor or major component in association with Mn in six other samples. A single piece is richer in calcite than in manganese oxide (CG84). All pieces exhibit concretions featuring more or less visible, mostly fibrous-shaped crystals, and variable frequency of pores and quartz inclusions. The smoothed bright patina evident on some specimens can be interpreted as the cortex of pedogenic nodules.

Hierarchical clustering based on SEM-EDS data (Fig. 4) identifies four clusters of mineral phases: Mn to Mn-Ba-rich phases, Mn-Fe-rich phases, Al-rich phases and a Si-rich phase (quartz) (see also Table SI 2; Fig. SI 2). The proportion of each mineral cluster in each archaeological sample distinguishes at least three groups: group I includes samples with variable content of Mn and Mn-Ba phases; group II samples are rich in Mn-Fe-bearing phases (CG28 and 36), and group III samples are rich in Al-bearing phases (CG21 and 47) (see also Table SI 3). No clear difference is observed between pure manganese dioxides and Babearing manganese oxides. The majority of black mineral pigments belong to this group, with several pieces composed of almost pure manganese oxides. The two pieces from group III are also the richest in Co (Table SI 2).

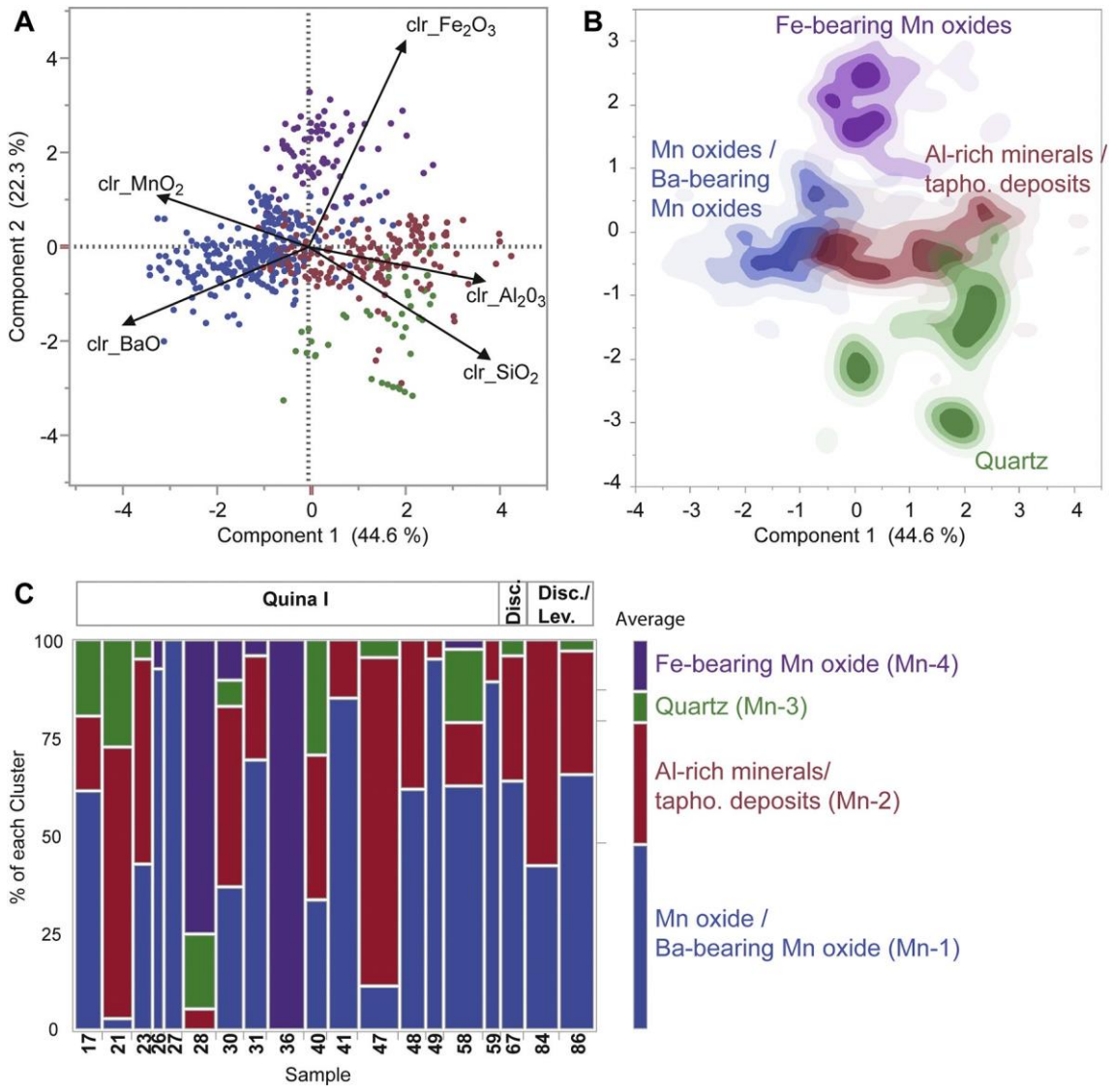

Fig. 4. Statistical treatment of SEM-EDS data (selected elements: Al_2O_3, SiO_2, MnO_2, Fe_2O_3 and BaO) of manganese oxide pieces. A: PCA showing the four main clusters of mineralogical composition. B: non-parametric distribution of the SEM-EDS data per cluster; the contours represent 100%, 75%, 50%, and 25% density. C: Percentages of each cluster in each sample; the width of the bars reflects the number of measurements.

4.1.2. Raw material provenance

The two pieces from Al and Co-rich group III probably share a similar geological origin. Lithiophorite is an oxidation product of hydrothermal or sedimentary ore of manganese deposits (i.e. wad) (Anthony et al., 2001). This mineral is currently unknown in the area around the site, the manganese outcrops from north of Nontron to south of Thiviers, or in the karstic crusts around Sarlat (Lougnon, 1981; Pitarch Martí and d'Errico, 2018). This could potentially be explained by the disappearance of this type of ores from the current landscape due to weathering, erosion, or mining activities. Mn-Fe-bearing pieces from group II could have a local origin, as the region is rich in iron oxide concretions. One Mn-rich outcrop is reported < 5 km north from the site (Le Theil) and not far from where we recorded iron oxide nodules (Pitarch Martí and d'Errico, 2018; Fig. 1). A third possibility could be outcrops around Sarlat, < 10 km from the site, which, based on PIXE analyses, are currently the most iron-rich manganese oxide outcrop in the region (Pitarch Martí and d'Errico, 2018). The origin of pure pyrolusite pieces or Ba-bearing manganese oxides is more difficult to identify. The presence of pedogenic cortex could indicate that they derive from a weathering profile. They could result from the

weathering of pre-existing manganese oxide deposits in the region. Difficulties in identifying their source could also be connected to these materials having been heavily exploited if not exhausted by 19th century mining operations (Lougnon, 1981).

4.1.3. Raw material processing

About 60% (n = 28) of the black manganese oxides bear traces of modification in the form of facets overlain by striations (Table 4). Most facets are irregular and, in some cases, concave in section. The presence of intersecting striations (Fig. 5A to D) suggests the facets were scraped with the edge of a thin blade or flake rather than abraded on a grindstone. These features are present on 42% of black pieces, while no less than14% present flat or convex facets covered by sub-parallel striations indicating that they were abraded on a grindstone (Fig. 5E to H). The distinction between the two processing technique is not always possible (5%), and the presence itself of the striations is sometimes questionable (5%). On > 50% (N = 14) of the striated pieces, striations appear smoothed, and some striated facets exhibit a bright lustre covering the striations (N = 6; 21%). Numerous fragments exhibit fractures, although none are clearly diagnostic of intentional knapping or crushing.

	No traces	%	Possible striations	%	Grinding	%	Grinding/scraping	%	Scraping	%	Total
Mn oxides[a]	15	34.9	2	4.7	6	14.0	2	4.7	18	41.9	43
Fe oxides[a]	25	100.0	0	0.0	0	0.0	0	0.0	0	0.0	25
Calcite, chalk	4	100.0	0	0.0	0	0.0	0	0.0	0	0.0	4
Total	44	61.1	2	2.8	6	8.3	2	2.8	18	25.0	72

Table 4 Number and percentages of pieces with striations resulting from grinding and/or scraping.

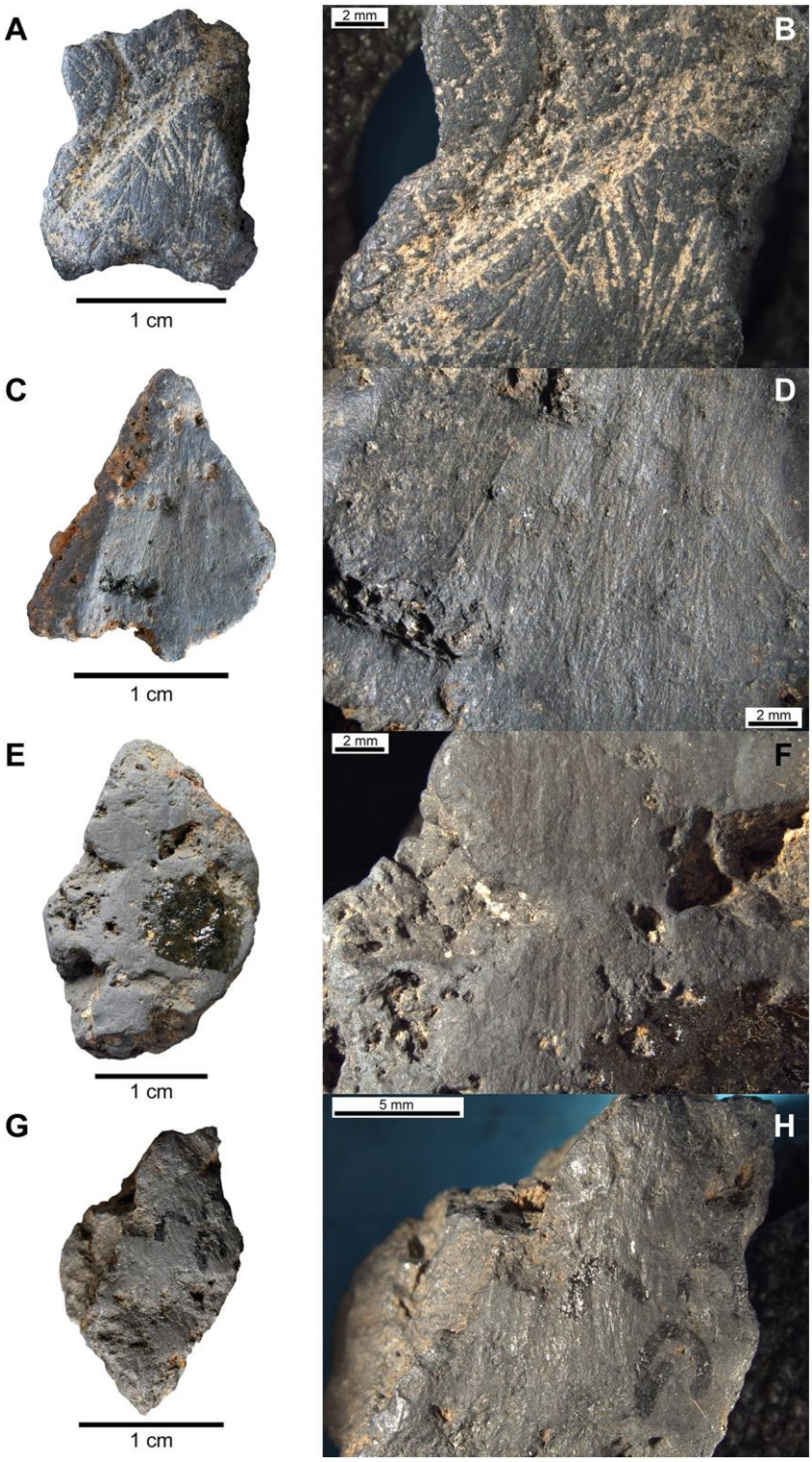

Fig. 5. Types of modification recorded on the Combe-Grenalcolouring materials. A: scraping; B: scraping and lustre; C: grinding; D: grinding and/or scraping and lustre.

No consistent association is observed between processing techniques and raw material type. The presence of a bright lustre is, on the other hand, preferentially observed on pieces associating Fe and Mn oxides. Four of the six lustred pieces contain Fe-rich phases (CG28, 31, 36 and 58; see Fig. 4), suggesting a different function compared to pieces that lack this feature. One of these pieces, CG31, is special in a number of regards. Two scraped faces bear a heavy, bright lustre (Fig. 6A and B) and one shows a cluster of small, aligned depressions (Fig. 6D). These last traces are similar to those identified archaeologically on bone (Patou-Mathis and Schwab, 2002; Verna and d'Errico, 2011) and stone (Archambault De Beaune, 1997) and produced experimentally on bone fragments used to retouched stone tools (Mallye

et al., 2012). This piece also presents a deep groove on an edge adjacent to a sharp fracture (Fig. 6A and C) and may reflect the use of a string to suspend the object. Grooves for the suspension of ornaments are known from early Upper Palaeolithic sites such as Grotte-du-Renne (Yonne, France) (Julien et al., 2017) and Les Cottés (Vienne, France) (Rigaud et al., 2014). Here, however, a part of the original piece is missing, making it difficult to reach a firm conclusion concerning its potential suspension.

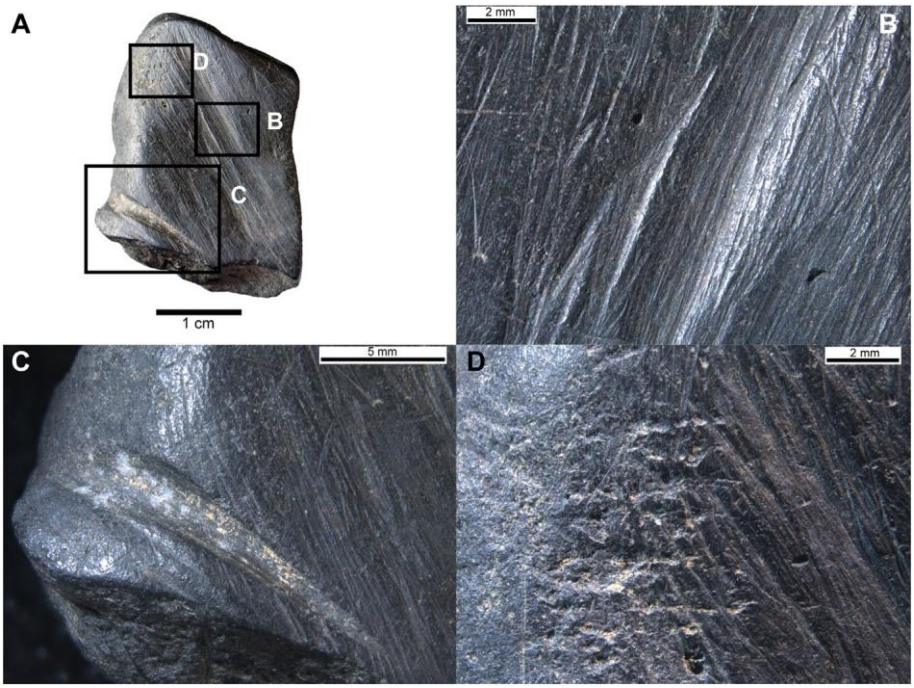

Fig. 6. Traces of modification on manganese oxide fragment CG31. A: striations from scraping covered by a bright lustre. B: Notch on an edge. C: traces of modification due to a use as a retoucher.

4.2. Yellow to red colouring materials

4.2.1. Raw material composition

The yellowish and reddish materials were grouped together, as distinguishing pieces that contain goethite (yellow streak) from those containing hematite (red streak) was not always possible. Their composition is summarized in Table 3 and detailed results are provided in Tables SI 2 and 3. While goethite is the most frequent phase identified, hematite (αFe_2O_3) is also present, along with calcite and quartz. Calcite is found either as deposits or as a substrate (limestone) for iron oxide deposits. SEM-EDS analyses indicate clay minerals (Si and Al) to be almost certainly present. The Fe-bearing materials mostly take the form of concretions or variably porous and quartz-rich sandstones. Several nodules exhibiting a bright cortex were also identified.

Hierarchical clustering based of SEM-EDS data (Fig. 7) identifies four clusters of mineral phases: pure iron oxides; Mn-bearing iron oxides; a Ca-rich phase associated to other minerals (calcite + clay minerals/sediment deposits); a Si rich phase (quartz) (see Table SI 2; Fig. SI 3). Contrary to what is observed with Mn phases, the proportion of each mineral cluster in each archaeological piece does not identify discrete groups. This heterogeneity can result from phases, such as calcite and alumina-silicates, acquired post-depositionally as a thin film on the surface of the objects.

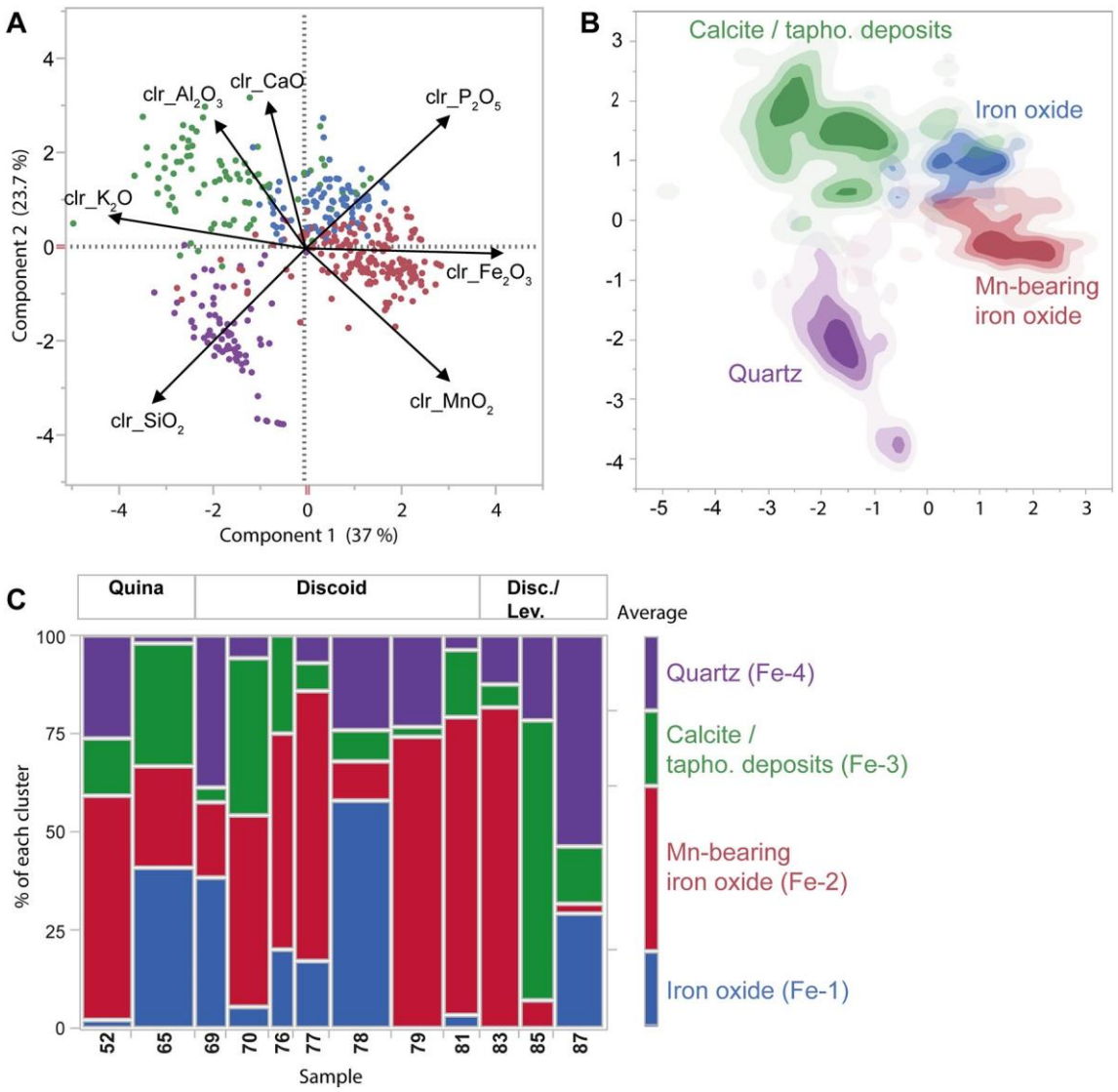

Fig. 7. Statistical treatment of SEM-EDS data for iron oxides (selected elements: Al_2O_3, SiO_2, P_2O_5, K_2O, CaO, MnO_2, Fe_2O_3). A: PCA showing four main clusters of mineralogical composition. B: non-parametric distribution of the SEM-EDS data per cluster; contours represent 100%, 75%, 50%, and 25% density. C: Percentages of each cluster within each sample; the width of the bars reflect the number of measurements.

4.2.2. Raw material provenance and selection

A comparison of the elemental composition of the archaeological iron oxide pieces with the geological samples shows that the archaeological pieces are not concretions derived from nearby unaltered limestone (Fig. 8; raw data in Table SI 4). Their elemental composition better matches nodules and, to a lesser degree, concretions from alterites. These latter two sources are difficult to distinguish regardless the data transformation employed. The PCAs of the alr values revealed a clear correspondence between the archaeological pieces and all local nodule sources (< 5 km) (Fig. 8B). The results of clr values are more ambiguous (Fig. 8A), as several measurements on archaeological pieces do not match with our geological assemblage. This may be due to a Ca content that partly derives from sediments adhering to the pieces or to the small size of the geological sample. Alr, on the other hand, have been shown to more accurately reflect the original geochemical signature of a source than does raw data (Popelka-Filcoff et al., 2007; Eiselt et al., 2011; Dayet et al., 2016). The same limitations of raw data might equally to clr. If only the PCA test using alr values is retained, a local origin for the iron oxide pieces appears most likely.

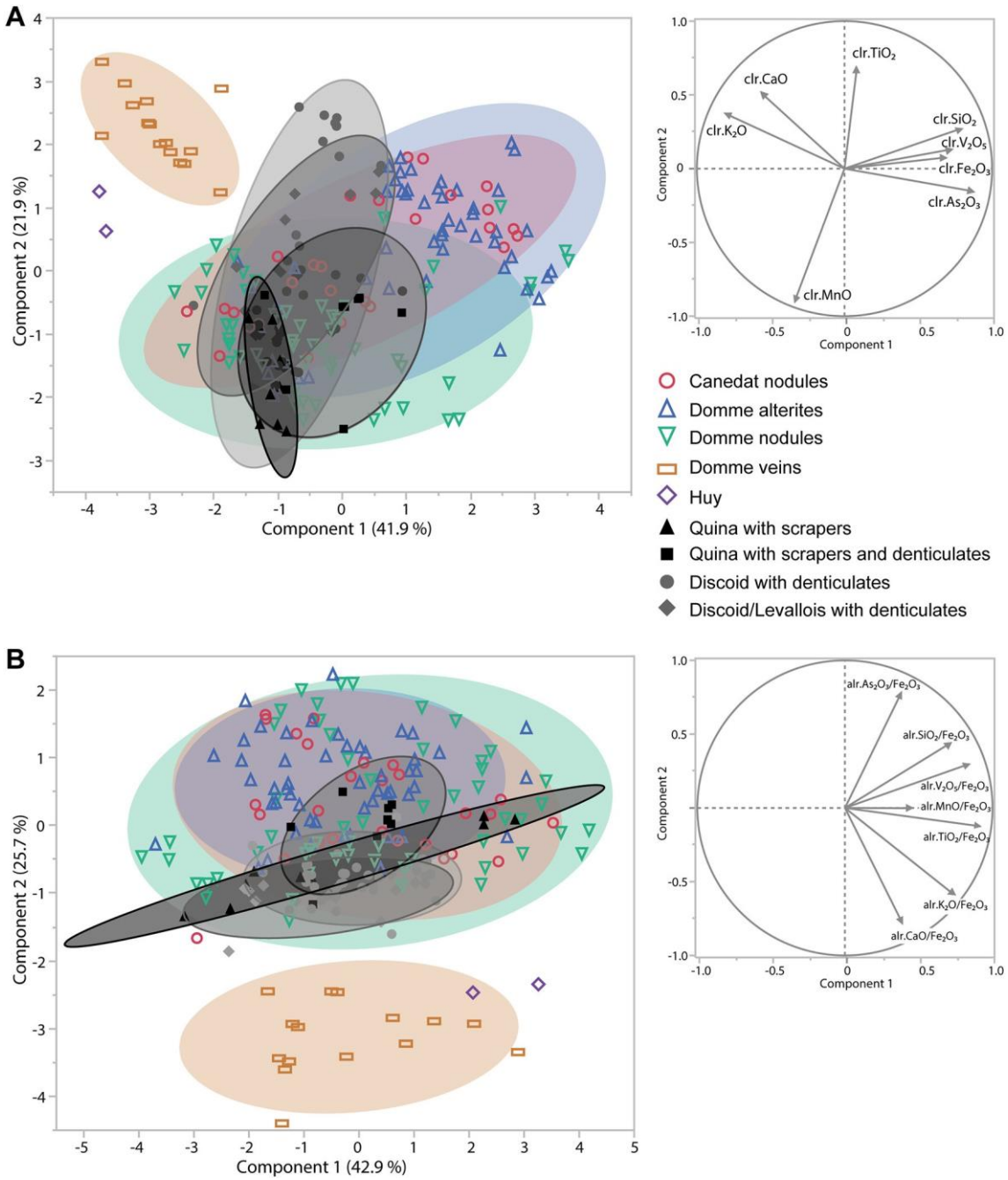

Fig. 8. PCA of pXRF data (selected elements: SiO_2, Fe_2O_3, MnO, CaO, K_2O, TiO_2, V_2O_5, As_2O_3) obtained on archaeological and geological iron oxides. A: clr data; B: alr data (ratio to Fe_2O_3). Note the strong heterogeneity of natural outcrops compared to archaeological specimens. Ellipses represent the normal density (p = .90).

Two interesting features emerge from the alr treatment when samples are grouped by LTC. Iron oxide pieces from the Quina layers cluster separately from those found in Discoid and Discoid/Levallois layers (Fig. 8B). Iron oxide data from the latter cluster together in the PCA and their compositional variability is low despite the high number of measurements. This may be due to their homogeneous content in Ca, K and Ti.

4.2.3. Raw material processing

Unlike manganese oxides, the iron oxides exhibit no traces of modification in the form of facets and striations. Most pieces exhibit fractures but none shows diagnostic features of intentional fragmentation or crushing (i.e. impact points, flake scars). While the morphology of two pieces is reminiscent of a

knapped flake, their smoothed edges, probably due to taphonomic processes, prevents drawing a definitive conclusion.

4.3. White mineral pigments

Four chalk fragments were identified among the lithics recovered by Bordes from layers 26 to 11. SEM-EDS analyses indicate that they are composed of a fine-grained calcite (Table 3). This material, absent in the Coniacian limestone in which the rock-shelter developed, is therefore potentially of a exogenic origin. However, in the absence of any evidence of human modification, their use as colorants is difficult to establish.

4.4. Stratigraphic distribution

The stratigraphic distribution of mineral pigments reveals interesting trends (Fig. 9): 1) manganese oxides are most frequent in layers 25 to 22; 2); a decrease in the frequency of mineral pigments is observed inlayer 21 to 18;3) iron oxide dominate the top of the sequence (layer 17 to 11). The absence of mineral pigments in layer 13, 18 and 19 may be an artefact of Bordes stratigraphy, as these layers are thin lenses that yielded much less material compared to the other levels from the upper third of the sequence (Faivre, 2008). In contrast, the recovery of a single mineral pigment in layer 20 is interesting considering the higher proportion of lithic artefacts found in this level.

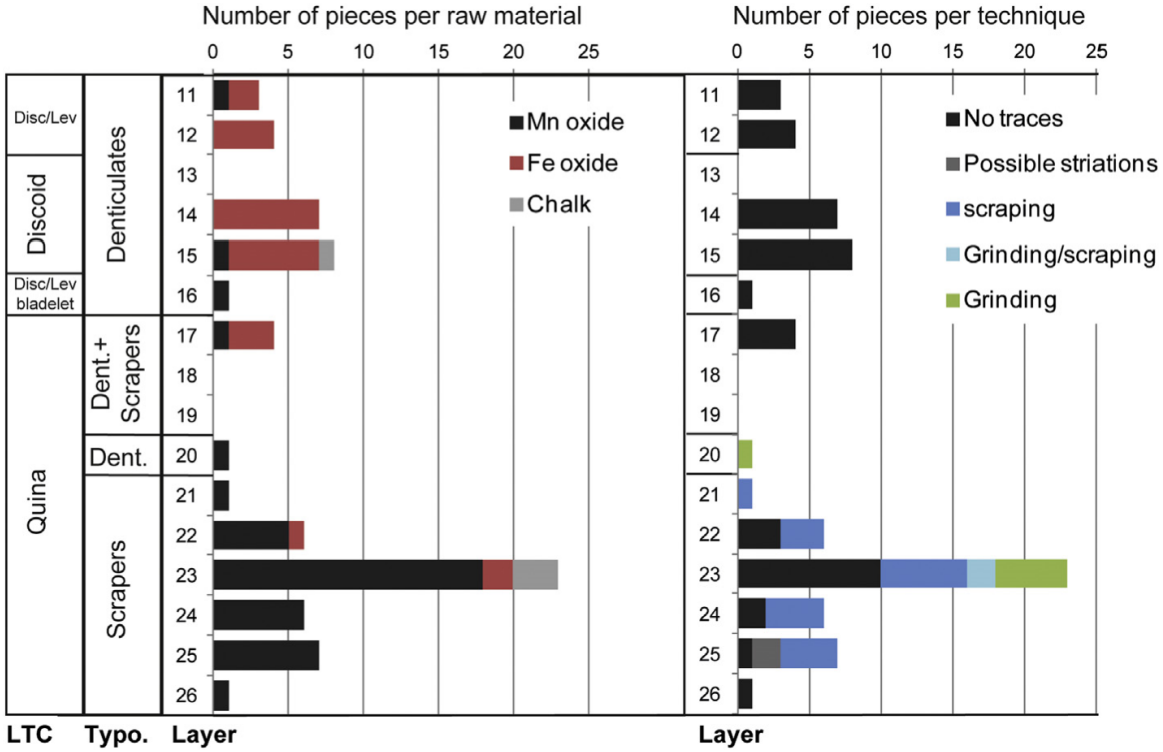

Fig. 9. Stratigraphic distribution of mineral pigments by raw material and traces of modification. LTC: lithic techno-complex.

Substantial differences can equally be observed between layers in terms of mineral pigment processing techniques (Fig. 9): scraped and ground pieces are found uniquely in layers 25 to 20. This is partly due to the absence of traces of modification on iron oxide pieces and the fact that the few manganese pieces from layers 19 to 11 also exhibit no traces of modification.

Changes between layers in mineral pigment preferences correlate to some extent with techno-typological changes in lithic industries. The decrease in mineral pigments frequency in the middle of the sequence coincides with a change in the typological composition of the Quina layers, with scrapers being dominant in layers 26 to 21 and denticulate in layer 20. The highest frequency of iron oxides coincides

with end of the Quina LTC. Moreover, the elemental composition of iron oxide pieces from these layers differs slightly from what was documented for pieces from the Discoid and Discoid/Levallois LTCs (see Section 4.2.2, Fig. 8). There is, in contrast, a clear overlap in the composition of red to yellow pieces found in the two last LTCs.

A Fisher's exact test of the frequency of mineral pigments within the Combe-Grenal stratigraphy rejected the null hypothesis that their stratigraphic distribution could result from random natural accumulation or random introduction of mineral pieces by the Neanderthal groups who occupied Combe-Grenal ($p = .000001$ after 1 million randomizations).

5. Discussion

5.1. Variations in pigment exploitation throughout Combe-Grenal deposits

Our technological, chemical and mineralogical analysis of a larger sample of pigments from Combe-Grenal reveals the use of black manganese oxides and the possible use of iron oxide and chalk. The introduction of black manganese oxides to the site by Neanderthals is indisputable. No pigment sources are found in the immediate vicinity of the site, which demonstrates the transport if not curation of these mineral-rich rocks that exhibit clear traces of scraping or grinding. Characterized by high concentrations in manganese oxides, mostly pyrolusite, the provenance of these materials is, however, still unknown, although a local source cannot be ruled out. Based on their composition, our results suggest that the Neanderthals groups who occupied Combe-Grenal exploited either three different types or three different sources of manganese-rich materials, or perhaps, a combination of the two. Extracted powders may have been used for different functions, including as an accelerant for igniting fires or as a tinting material. Although scraping and grounding are compatible with both uses, the smoothed aspect of the striations is more consistent with the hypothesis that manganese oxides were rubbed on human skins or animal hides, similar to what had previously been proposed for the Pech-de-l'Azé I pigments (Soressi and d'Errico, 2007). The presence of impact marks suggesting the use of one piece as a retoucher, the coexistence of both grinding and scraping, and the identification of three types of manganese-rich materials equally argue in favour of the Combe-Grenal pigments having served multiple purposes. The retoucher, which also exhibits traces of scraping, perfectly illustrates the multifunctional nature of the Combe-Grenal pigments. Moreover, the likelihood of it be curated is potentially illustrated by a groove that may have served to suspend the piece.

The absence of diagnostic human modifications on the iron-rich rock fragments raises the question of whether they were introduced to Combe-Grenal by Neanderthals. The on-going geoarchaeological study of the sequence shows that exogenous materials played a negligible role in the accumulation of layers 16 to 14, where most of the red oxide pieces were found (Lenoble, personal communication). The inclusion of exogenous materials was apparently greater during the accumulation of layers 23 to 17, where the frequency of iron oxide is very low. Other elements equally support a human origin for the iron-rich rocks found at Combe-Grenal. The pXRF analysis of these objects revealed slight differences in elemental composition between iron oxides pieces from the bottom (layers 26 to 17) and top of the sequence. Additionally, the iron oxides from the Discoid and Discoid/Levallois techno-complexes exhibit a particularly low variation in elemental composition compared to geological sources. Both observations argue in favour of the Neanderthal groups who occupied Combe-Grenal to have preferred certain sources or types of iron-rich minerals.

Visual similarities between dark manganese and dark iron oxide pieces could explain the presence of the latter in the Quina LTC. However, unlike the manganese oxide pieces, none of dark iron oxide pieces bear evidence of scraping. This suggests that Quina groups were well aware of differences in the composition and hence properties of the Mn- and Fe-rich minerals, and used them for different functions. The consistent gathering of iron oxide pieces with red and yellow hues within the Discoid and Discoid/Levallois LTCs is consistent with the idea that they were collected to produce red to yellow

powders. How powder was produced and for what end remains unclear. The absence of traces of modification argues in favour of crushing and pounding. The presence of both goethite and hematite that produce a yellow to brown and red powder, respectively, raises the question of whether red, yellow, brown or all three colours were actively sought by Neanderthal groups. Goethite-bearing nodules may have been found in higher proportions at the site because they were less valued than hematite-bearing materials and therefore more frequently abandoned on the site. Visual similarities between the raw (i.e. unprocessed) forms of the two pigments forms may explain why numerous goethite–rich fragments were discarded, and could further support the idea that hematite-rich red powders were preferred over goethite-rich yellow ones.

Variations in manganese and iron oxide pieces across the sequence are one of the most interesting patterns we found. While the null hypothesis of a random accumulation of iron and manganese oxides within the sequence is highly unlikely ($p < .01$), potential biases induced by Bordes' excavation methods cannot be ruled out. For example, a recent comparison of Bordes' faunal assemblage with material recovered during on-going excavations revealed substantial recovery biases (see Discamps and Faivre, 2017 for more details). However, the selection by excavators of one type of oxide over the others appears highly unlikely - both types of colouring materials were recognised from the outset of Bordes' excavations. Moreover, our sorting of the unwashed material collected during Bordes' excavation produced only a few mineral pigments, which were either manganese or iron-rich. Several small and unmodified pieces in the collection also demonstrate that particular care was taken in identifying pigments during excavations (see Table 1). Although this does not absolutely rule out a bias for larger, modified pigments, a preliminary examination of the mineral pigments recovered from the 2015 to 2018 excavations produced no pure forms of manganese oxides from stratigraphic units that are the equivalent of Bordes' layers 12 to 16 (for details of stratigraphic correlations see Discamps et al., 2016; Discamps and Faivre, 2017). On the other hand, iron oxide pieces were recovered from these layers, corroborating our data from Bordes' pigment assemblage. Taken together, this suggests that trends in mineral pigment frequency and type most likely reflect intentional choices by Neanderthal groups and not excavation biases.

The low frequency of iron oxide pieces in the Quina LTC, combined with the absence of scraping traces, is at odds with the data obtained from the SEM-EDS residue analysis carried out by Beyries and Walter (1996), who identified iron oxides on seven Quina scrapers. They put forward the hypothesis that these scrapers were used to process iron oxides. They advised to look for scraped iron oxide pieces within the Quina layers in order to validate their hypothesis. This is what we did and we found none. A possible explanation for this absence is that they were modified at another site, with the scrapers subsequently transported and ultimately discarded at Combe-Grenal.

5.2. Mineral pigments: Proxies for cultural identity in Neanderthal societies?

Most of the debate surrounding the significance of Lower and Middle Palaeolithic/Stone Age mineral pigments revolves around the issue of their use in symbolic practices (Marshack, 1981; McBrearty and Brooks, 2000; Watts, 2002, 2009, 2010; Henshilwood et al., 2002; Salomon, 2009; Zilhão et al., 2010; d'Errico and Stringer, 2011; d'Errico et al., 2012). Of equal importance is the potential use of these materials to actively signal cultural identity or group membership. This question is particularly relevant in the context of the still unresolved debate concerning the relative importance of function versus culture in the description of late Middle Palaeolithic industrial variability. For an artefact to be a cultural marker, it is not necessary that it plays a symbolic function or reflects 'active style' (Sacket, 1982; Sackett, 1986; Chase, 1991). It can simply have an indexical property (Peirce, 1932), whose particular traits are independent of raw material, technological or functional constraints (Chase and Dibble, 1987; Chase, 1991), and therefore reflect a cultural choice specific to a particular human group. The use of such an item creates an enduring link between the object and the group: the object is perceived by the members of the group as naturally identifying the group without any explicit desire of group members to differentiate themselves from a neighbouring group.

Did the different Neanderthal groups at Combe-Grenal use mineral pigments in exactly this way? Recorded variations in mineral pigment use through time are difficult to attribute to environmental changes limiting access to particular raw material sources. Our results suggest that both manganese and iron oxides were available around CombeGrenal throughout the accumulation of the sequence. The lower proportion of manganese oxides at the top of the sequence could potentially reflect increased vegetation restricting access to manganese sources. While available data from small vertebrates does suggest minor environmental changes concomitant with the beginning of the Discoid/ Levallois LTC (Marquet, 1989), the decrease in manganese oxide use clearly predates this event, which rules out environmental change as a factor. In addition, the fact that three different Upper Palaeolithic groups (Aurignacian, Solutrean, Magdalenian) encompassing numerous climate changes also employed manganese and iron oxides in the region (Chalmin et al., 2003; Beck et al., 2014; Pitarch Martí and d'Errico, 2018) corroborates the view that climate changes did not substantially affect access to mineral pigment sources. Testing the hypothesis that changes in mineral pigments are not due to shifts in function is more complex due to the absence of traces of modification on iron oxides. However, the variety of processing techniques and use-wear patterns on manganese pieces, including their occasional use as retouchers, plead in favour of these materials to have likely fulfilled multiple functions. In the absence of substantial concomitant shifts in subsistence strategies, this pattern would be consistent with the hypothesis that function alone does not explain the observed trend in pigment use. With that said, the fact that the decrease in manganese oxide use within the Quina levels accompanies a change in stone tool typology could reflect a general change in site function. However, the diversity of manganese oxide uses that we highlighted may also include a cultural dimension. In other words, differences in pigment use may reflect changes in how Neanderthal groups perceived each other. Additional use-wear analyses of lithic materials are however necessary to further test this hypothesis.

In parallel, can the association between flake production systems and the use of particular mineral pigments be interpreted as the ‘signature’ of different cultural groups? At Combe-Grenal, manganese oxide is abundant in Quina LTC levels and iron oxides in the Discoid and Discoid/Levallois LTCs levels. In south-western France, however, the use of manganese oxide is not restricted to the Quina LTC (Table 5). Clear evidence of its use is found in layers attributed to Bordes' Mousterian of Acheulean Tradition (MTA) at Pech-de-l'Azé I (layer 4; Demars, 1992; Soressi and d'Errico, 2007), in association with Levallois flaking systems at Caminade-Est (layer M2; de Sonneville-Bordes, 1969) and Pech de l'Azé IV (layer I and J), or in association with Discoid flaking systems at Le Moustier (Demars, 1992) and Pech de l'Aze IV (Demars, 1992; Turq et al., 2011). Red iron oxides are, instead, present in the Quina level of La-Chapelle-aux-Saints (Demars, 1992). One of the most secure cases of mineral pigment use associated with the Discoid LTC comes from level H of Le Moustier, Dordogne (Peyrony, 1921; Demars, 1992; Pitarch Martí and d'Errico, 2018). While iron oxides are absent from this layer, black manganese oxide fragments are found in association with an exclusively discoidal lithic assemblage dominated by notches and denticulates throughout a 1.2 m-thick layer. The Discoid LTC from Combe-Grenal is equally dominated by these tool types. Finally, about 80 pieces of red and/or yellow iron concretions, six of which exhibit traces of modification, were discovered in two pits containing typical discoidal artefacts at the open-air site of Ormesson, in the Paris Basin, Seine-et-Marne, France (Bodu et al., 2014).

Site	Layers/levels	Bordes' facies	LTC after revision (Flaking system)	Typology after revision	Mineral pigments Nature	References
Charente						
La Quina	Moustérien supérieur'	MTA	?	?	Mostly Mn oxide	Martin, 1923
Corrèze						
La-Chapelle-aux-Saints	?	Quina	?	?	Fe oxide	Demars, 1992
Dordogne						
Combe Grenal	12-16	Denticulates	Discoid, Discoid/ levallois	Denticulates	Mostly Fe oxide	Demars, 1992; Faivre et al., 2014; This study
	26-17	Quina		Scrapers and denticulates	Mostly Mn oxide	Demars, 1992; Faivre et al., 2014; This study
Le Moustier	H	MTA	Discoid	Denticulates	Mostly Mn oxide	Demars, 1992; Gravina and Discamps, 2015
	G3-G4	MTA	Bifacial	Bifacial pieces	Mostly Mn oxide	Demars, 1992; Gravina, 2017
	G1-G2	MTA	Levallois	Bifacial pieces	Mostly Mn oxide	Demars, 1992; Gravina, 2017
Pech de l'Azé I	4	MTA	Bifacial	Bifacial pieces	Mostly Mn oxide	Demars, 1992; Soressi and d'Errico, 2007
Pech de l'Azé IV	F	MTA	Discoid	?	Mostly Mn oxide	Demars, 1992
	I-J	Typical Mousterian	Levallois?	?	Mostly Mn oxide	Demars, 1992
Caminade	3b-2	La Ferrassie Mousterian	Levallois?	?	Mostly Mn oxide	de Sonneville-Bordes 1969; Demars, 1992

Table 5 Mousterian sites in south-western France with reliable evidence (more than two pieces, secure attribution to a lithic techno-complex) for mineral pigments reported in the literature and associated lithic assemblages characteristics.

In sum, we currently have no unambiguous evidence for a one to one correspondence between mineral pigment and lithic technology at a regional level. This may be due to the fact that layers from different sites and similar lithic assemblages are not contemporaneous, that mineral pigments use was conditioned by economic rather that cultural constraints or that they fulfilled indexical, or even symbolic functions, independent of the technological tradition of a particular group. Better chronological resolution, the reappraisal of key Middle Palaeolithic lithic assemblages, and a more detailed analysis of mineral pigment are needed to tease apart these hypotheses.

6. Conclusion

Middle Palaeolithic mineral pigment use remains both a limited and highly localised phenomenon compared to the much more substantial behavioural record from Neanderthal stone tool technologies and subsistence practices. Our results from Combe-Grenal nevertheless highlight the interest of including variations in pigment selection and use for the definition of Neanderthal material culture patterning. Our detailed analysis of the Combe-Grenal pigment assemblage revealed the intense use of black manganese oxides, the very probable use of yellow to red iron oxides, and the potential use of white chalk. A clear stratigraphic trend in raw materials types and colours was also observed. Black manganese oxides are most abundant in the lower Quina layers, and then drastically decrease in the uppermost part of this LTC; yellow red iron oxide pieces are dominant from the end of the Quina LTC and throughout the Discoid and Discoid/Levallois LTCs. The decrease in manganese oxide use within the Quina LTC might mark some kind of cultural change. Further work on mineral pigment collections, especially those from the Quina and the Discoid LTCs, will shed further light on Neanderthal cultural traditions. Interdisciplinary approaches similar to the one developed here will undoubtedly open new perspectives for deciphering the cultural significance of the Mousterian archaeological record in both south-western France and further afield.

Acknowledgements

We would like to thank the Musée National de la Préhistoire at Les Eyzies, particularly the director, J.-J. Cleyet-Merle, for permission to study the pigments from Bordes' excavations at Combe-Grenal, as well as P. Jacquement and N. Bernard. We would also like to thank A. Gibaud for help with the pXRF measurements, Y. Lefrais (IRAMATCRP2A) for help with the SEM-EDS analyses, and F. Santos (PACEA, University of Bordeaux) for help with the statistical tests. We are grateful to the reviewers for their insightful comments that contributed to the improvement of the manuscript. This research was funded by the LabEx LaScArBx, a research programme depending on the French institution ANR (ANR-10-LABX-52). The research presented here was initiated during the "NéMo" (Néandertal face à la mort, culture/pratiques funéraires) LabEx project at the University of Bordeaux (Dirs. Jean-Philippe Faivre, Christelle Lahaye, and Bruno Maureille) and finalized in the course of the LaScArBx (ANR-10-LABX-52) project "The earliest use of pigment in South-West France" led by Francesco d'Errico and the NATCH (Neanderthalenses Aquitanensis: Territoires, Chronologie, Humanité) project financed by the Aquitaine Region, France (Dir. J.-P. Faivre).

This work was partly supported by the Research Council of Norway through its Centre's of Excellence funding scheme, SFF Centre for Early Sapiens Behaviour (SapienCE), project number 262618.

References

Aitchison, J., 1986. The Statistical Analysis of Compositional Data. Monographs on Statistics and Applied Probability. Chapman & Hall Ltd., London (UK) (416 p).

Anderson-Gerfaud, P., 1981. Contribution méthodologique à l'analyse des microtraces d'utilisation sur les outils préhistoriques. Thèse de 3ème cycle. Université de Bordeaux (314 pp).

Anthony, J.W., Bideaux, R.A., Bladh, K.W., Nichols, M.C., 2001. Handbook of Mineralogy. Mineralogical Society of America.ed, Chantilly, VA 20151–1110, USA.

Archambault De Beaune, S., 1997. Les galets utilisés au Paléolithique supérieur: approche archéologique et expérimentale. In: CNRS Éditions. XXXIIe supplément à Gallia Préhistoire, pp. 298.

Astruc, J.G., 1990. Carte géologique Gourdon (1/50 000) et notice, feuille 832. B.R.G.M, Orléans.

Audouin, F., Plisson, H., 1982. Les ocres et leurs témoins au Paléolithique en France: enquête et expériences sur leur validité archéologique. In: Cahiers du Centre de Recherches Préhistoriques. vol. 8. pp. 33–80.

Baffier, D., Girard, M., Menu, M., Pomiès, M.-P., Vignaud, C., 1999. La couleur à la Grande Grotte d'Arcy sur Cure(Yonne). L'Anthropologie 103, 1–22.

de Balbín Behrmann, R.D., González, J.J.A., 2009. Les colorants de l'art paléolithique dans les grottes et en plein air. L'Anthropologie 113, 559–601.

Beck, L., Rousselière, H., Castaing, J., Duran, A., Lebon, M., Moignard, B., Plassard, F., 2014. First use of portable system coupling X-ray diffraction and X-ray fluorescence for in-situ analysis of prehistoric rock art. Talanta 129, 459–464.

Beyries, S., 1987. Variabilité de l'industrie lithique au Moustérien. Approche fonctionnelle sur quelques gisements français. BAR International Series 328 Archaeopress, Oxford (204 pp).

Beyries, S., Walter, P., 1996. Racloirs et colorants à Combe-Grenal: Le problème de la retouche. Quina. Quaternaria Nova VI, 167–185.

Binford, L.R., 1983. Interassemblage variability: The Mousterian and the functional argument. In: Binford, Lewis Roberts (Ed.), Working at Archaeology. Academic Press, New York, pp. 131–153.

Binford, L.R., Binford, S.R., 1966. A preliminary analysis of functional variability in the Mousterian of Levallois Facies. Am. Anthropol. 68, 238–295.

Bodu, P., Salomon, H., Leroyer, M., Naton, H.-G., Lacarriere, J., Dessoles, M., 2014. An open-air site from the recent Middle Palaeolithic in the Paris Basin (France): les Bossats at Ormesson (seine-et-Marne). Quat. Int. 331, 39–59.

Bonjean, D., Vanbrabant, Y., Abrams, G., Pirson, S., Burlet, C., Di Modica, K., Otte, M., Vander Auwera, J., Golitko, M., McMillan, R., Goemaere, E., 2015. A new Cambrian black pigment used

during the late Middle Palaeolithic discovered at Scladina Cave (Andenne, Belgium). J. Archaeol. Sci. 55, 253–265.
Bordes, F., 1955. La stratigraphie de la Grotte de Combe-Grenal, commune de Domme (Dordogne) Note préliminaire. Bulletin de la Société préhistorique de France 52, 426–429.
Bordes, F., 1972. A Tale of Two Caves. Harper and Row, New York.
Bourguignon, L., Faivre, J.-P., Turq, A., 2004. Ramification des chaînes opératoires: une specificité du Mousterien? Paléo 16, 37–49.
Capdeville, J.-P., Rigaud, J.P., 1987. Carte géologique 1/50 000 de Sarlat - La Canéda et notice explicative, feuille 808. B.R.G.M, Orléans.
Chalmin, E., Menu, M., Vignaud, C., 2003. Analysis of rock art painting and technology of Palaeolithic painters. Meas. Sci. Technol. 14, 1590–1597.
Chase, P.G., 1991. Symbols and paleolithicartifacts: style, standardization, and the imposition of arbitrary form. J. Anthropol. Archaeol. 10, 193–214.
Chase, P.G., Dibble, H.L., 1987. Middle paleolithic symbolism: a review of current evidence and interpretations. J. Anthropol. Archaeol. 6, 263–296.
Clément, S., 2014. Recyclage au Paléolithique moyen. Bulletin la Société préhistorique française 131–134.
Clottes, J., Menu, M., Walter, P., 1990. La préparation des peintures magdaléniennes des cavernes ariégeoises. Bulletin dela Société Préhistorique Française 87, 170–192.
Comas-Cufí, M., Thió-Henestrosa, S., 2011. CoDaPack 2.0: A stand-alone, multi-platform compositional software. In: Egozcue, J.J., Tolosana-Delgado, R., Ortego, M.I. (Eds.), CoDaWork'11: 4th International Workshop on Compositional Data Analysis. Sant Feliu de Guíxols.
Couraud, C., 1988. Pigments utilisés en Préhistoire, provenance, préparation, mode d'utilisation. L'Anthropologie 82, 17–28.
Dayet, L., Texier, P.-J., Daniel, F., Porraz, G., 2013. Ochre resources from the Middle Stone Age sequence of Diepkloof Rock Shelter, Western Cape, South Africa. J. Archaeol. Sci. 40, 3492–3505.
Dayet, L., d'Errico, F., Garcia-Moreno, R., 2014. Searching for consistencies in Châtelperronian pigment use. J. Archaeol. Sci. 44, 180–193.
de Sonneville-Bordes, D., 1969. Manganèse raclé dans le moustérien de type Ferrassie de Caminade-Est. Quaterneria XI, 111–114.
Dayet, L., Le Bourdonnec, F.-X., Daniel, F., Porraz, G., Texier, P.-J., 2016. Ochre provenance and procurement strategies during the Middle Stone Age at Diepkloof Rock Shelter, South Africa. Archaeometry 58, 807–829.
Delagnes, A., Meignen, L., 2006. Diversity of lithic production systems during the Middle Paleolithic in France. In: Hovers, E., Kuhn, S.L. (Eds.), Transitions Before the Transition: Evolution and Stability in the Middle Paleolithic and Middle Stone Age. Springer US, Boston, MA, pp. 85–107.
Demars, P.-Y., 1992. Les colorants dans le Moustérien du Périgord: l'apport des fouilles de F. Bordes. Bulletin de la Société préhistorique de l'Ariège 47, 185–194.
d'Errico, F., Stringer, C.B., 2011. Evolution, revolution or saltation scenario for the emergence of modern cultures? Philosophical Transactions of the Royal Society B: Biological Sciences 366 (1567), 1060–1069.
d'Errico, F., Garcia Moreno, R., Rifkin, R.F., 2012. Technological, elemental and colorimetric analysis of an engraved ochre fragment from the Middle Stone Age levels of Klasies River Cave 1, South Africa. J. Archaeol. Sci. 39 (4), 942–952.
Dibble, H.L., 1984. Interpreting typological variation of Middle Paleolithic scrapers: function, style, or sequence of reduction? J. Field Archaeol. 11, 431–436.
Dibble, H.L., 1987. The interpretation of Middle Paleolithic scraper morphology. Am. Antiq. 52 (1), 109–117.

Discamps, E., Faivre, J.-P., 2017. Substantial biases affecting Combe-Grenal faunal record cast doubts on previous models of Neanderthal subsistence and environmental context. J. Archaeol. Sci. 81, 128–132.

Discamps, E., Royer, A., 2017. Reconstructing palaeoenvironmental conditions faced by Mousterian hunters during MIS 5 to 3 in southwestern France: a multi-scale approach using data from large and small mammal communities. Quat. Int. 433, 64–87.

Discamps, E., Jaubert, J., Bachellerie, F., 2011. Human choices and environmental constraints: deciphering the variability of large game procurement from Mousterian to Aurignacian times (MIS 5-3) in southwestern France. Quat. Sci. Rev. 30, 2755–2775.

Discamps, E., Muth, X., Gravina, B., Lacrampe-Cuyaubère, F., Chadelle, J.-P., Faivre, J.-P., Maureille, B., 2016. Photogrammetry as a tool for integrating archival data in archaeological fieldwork: examples from the Middle Palaeolithic sites of Combe-Grenal, Le Moustier, and Regourdou. Journal of Archaeological Science: Reports 8, 268–276.

Eiselt, B.S., Popelka-Filcoff, R.S., Darling, J.A., Glascock, M.D., 2011. Hematite sources and archaeological ochres from Hohokam and O'odham sites in Central Arizona: an experiment in type identification and characterization. J. Archaeol. Sci. 38, 3019–3028.

Faivre, J.-Ph, 2008. Organisation techno-économique dessystèmes de production dans le Paléolithique moyen récent du Nord-estaquitain: Combe-Grenal et Les Fieux. vol. 1 Université Bordeaux Ph.D. thesis. (555pp).

Faivre, J.-Ph, 2011. Le «Moustérien à denticulés» de la couche 20 de Combe-Grenal: implications techniques, économiques et fonctionnelles au sein du système de production Quina en Périgord. PALEO 21, 135–162.

Faivre, J.-P., Discamps, E., Gravina, B., Turq, A., Guadelli, J.-L., Lenoir, M., 2014. The contribution of lithic production systems to the interpretation of Mousterian industrial variability in South-Western France: the example of Combe-Grenal (Dordogne, France). Quat. Int. 350, 227–240.

Faivre, J.-P., Discamps, E., Gravina, B., Turq, A., Bourguignon, L., 2017a. Cleaning up a Messy Mousterian: how to describe and interpret Late Middle Palaeolithic chronocultural variability in Atlantic Europe. Quat. Int. 433, 1–3.

Faivre, J.-P., Gravina, B., Bourguignon, L., Discamps, E., Turq, A., 2017b. Late Middle Palaeolithic lithic technocomplexes (MIS 5–3) in the northeastern Aquitaine Basin: advances and challenges. Quat. Int. 433, 116–131.

Geneste, J.-M., Jaubert, J., Lenoir, M., Meignen, L., Turq, A., 1997. Les moustérienscharentiens du Sud-ouest et du Languedoc oriental: approche technologique et variabilité géographique. Paléo 9, 101–142.

Gravina, B., 2017. Intra-level technological change and its implications for Mousterian assemblage variability. The example of Le Moustier, layer G. Quat. Int. 433, 132–139.

Gravina, B., Discamps, E., 2015. MTA-B or not to be? Recycled bifaces and shifting hunting strategies at Le Moustier and their implication for the late Middle Palaeolithic in southwestern France. J. Hum. Evol. 84, 83–98.

Guadelli, J.-L., Laville, H., 1990. L'environnement climatique de la fin du Moustérien à Combe-Grenal et à Camiac: confrontation des données naturalistes et implications. In: Paléolithique Moyen Récent et Paléolithique Supérieur Ancien En Europe. Ruptures et Transitions: Examen Critique Des Documents Archéologiques, Mémoires Du Musée de Préhistoire d'Ile-de-France. Farizy, C., Nemours, pp. 43–48.

Henshilwood, C.S., d'Errico, F., Yates, R., Jacobs, Z., Tribolo, C., Duller, G.A.T., Mercier, N., Sealy, J.C., Valladas, H., Watts, I., Wintle, A.G., 2002. Emergence of modern human behavior: Middle Stone Age engravings from South Africa. Science 295 (5558), 1278–1280.

Heyes, P.J., Anastasakis, K., de Jong, W., van Hoesel, A., Roebroeks, W., Soressi, M., 2016. Selection and use of manganese dioxide by Neanderthals. Sci. Rep. 6, 22159.

Hodgskiss, T., 2010. Identifying grinding, scoring and rubbing use-wear on experimental ochre pieces. J. Archaeol. Sci. 37, 3344–3358.

Hodgskiss, T., 2013. Ochre use in the Middle Stone Age at Sibudu, South Africa: grinding, rubbing, scoring and engraving. Journal of African Archaeology 11, 75–95.

Jaubert, J., 2011. Les archéoséquences du Paléolithique moyen du Sud-Ouest de la France: quel bilan un quart de siècle après François Bordes? In: F. Delpech et J. Jaubert (Dir.) François Bordes et la Préhistoire. Colloque international François Bordes, Bordeaux 22–24 avril 2009, Paris, Édit. du CTHS, p. 235–253.

Jaubert, J., 2014. Middle Palaeolithic archeo-sequences from southwestern France: Where do we stand a quarter century after François Bordes? In: Basic Issues in Archaeology, Anthropology, and Ethnography of Eurasia. Festschrift on the Occasion of Anatoly Derevianko's 70th Birthday. Novosibirsk, pp. 194–212.

Julien, M., d'Errico, F., Vanhaeren, M., 2017. Les Néandertaliens du Paléolithique supérieur. Parure et industries osseuses du Châtelperronien. In: Le troisième Homme, Préhistoire de l'Altaï. Les éditions Rmn-Grand Palais.

Lougnon, J., 1981. Les gisements de manganèse. In: Ressources minières française tome. BRGM, pp. 10.

Lucas-Tooth, H.J., Price, B.J., 1961. A mathematical method for the investigation of Interelement effects in X-ray fluorescence analysis. Metallurgia 64 (383), 149.

MacDonald, B.L., Fox, W., Dubreuil, L., Beddard, J., Pidruczny, A., 2018. Iron oxide geochemistry in the Great Lakes Region (North America): implications for ochre provenance studies. J. Archaeol. Sci. Rep. 19, 476–490.

Mallye, J.B., Thiébaut, C., Mourre, V., Costamagno, S., Claud, É., Weisbecker, P., 2012. The Mousterian bone retouchers of Noisetier cave: experimentation and identification of marks. J. Archaeol. Sci. 39 (4), 1131–1142.

Marquet, J.C., 1989. Paléoenvironnement et chronologie des sites du domaine atlantique français d'âge Pléistocène moyen et supérieur d'après l'étude des rongeurs. Ph.Dthesis. Université de Bourgogne, Dijon.

Marshack, A., 1981. On Paleolithic ochre and the early uses of color and symbol. Curr. Anthropol. 22 (2), 188–191.

Martin, H., 1923. Recherches sur l'Evolution du Moustérien dans le Gisement de La Quina (Charente), l'Industrie lithique. Imprimerie Ouvrière, Angoulême.

McBrearty, S., Brooks, A.S., 2000. The revolution that wasn't: a new interpretation of the origin of modern human behavior. J. Hum. Evol. 39 (5), 453–563.

Menu, M., 2009. L'analyse de l'art préhistorique. L'Anthropologie 113, 547–558.

Morin, E., Delagnes, A., Armand, D., Castel, J.-C., Hodgkins, J., 2014. Millennial-scale change in archaeofaunas and their implications for Mousterian lithic variability in Southwest France. J. Anthropol. Archaeol. 36, 158–180.

Patou-Mathis, M., Schwab, C., 2002. Fiche générale. In: Patou-Mathis, M. (Ed.), Retouchoirs, Compresseurs, Percuteurs Os à impressions et éraillures, Fiches de la Commission de Nomenclature sur l'Industrie de l'Os Préhistorique Cahier X. Éditions de la Société Préhistorique Française, Paris, pp. 11–19.

Peirce, C.S., 1932. The icon, index, and symbol. In: Hartshome, C., Weiss, P. (Eds.), Collected Papers of Charles SandersPierce, II. vol. 1960. Harvard University Press, Cambridge, MA, pp. 156–173.

Peyrony, D., 1921. Une pierre coloriée d'époque moustérienne. In: Compte-Rendu de La 44e Session, Strasbourg 1920. Association Française Pour l'avancement Des Sciences, Strasbourg, pp. 494–495.

Pitarch Martí, A., d'Errico, F., 2018. Seeking black. Geochemical characterization by PIXE of Palaeolithic manganese-rich lumps and their potential sources. J. Anthropol. Archaeol. 50, 54–68.

Popelka-Filcoff, R.S., Robertson, J.D., Glascock, M.D., Descantes, C., 2007. Trace element characterization of ochre from geological sources. J. Radioanal. Nucl. Chem. 272, 17–27.

Queffelec, A., D'Errico, F., Vanhaeren, M., 2017. Analyse des blocs de matière colorante de Praileaitz I (Deba, Gipuzkoa). In: Munibe Monographs. Anthropology and Archaeology Series, vol. 1. pp. 493–503.

Rifkin, R.F., 2011. Assessing the efficacy of red ochre as a prehistoric hide tanning ingredient. Journal of African Archaeology 9, 131–158.

Rifkin, R.F., 2012a. The Symbolic and Functional Exploitation of Ochre during the South African Middle Stone Age. University of Witwatersrand, Johannesburg.

Rifkin, R.F., 2012b. Processing ochre in the Middle Stone Age: testing the inference of prehistoric behaviours from actualistically derived experimental data. J. Anthropol. Archaeol. 31, 174–195.

Rigaud, S., Roussel, M., Rendu, W., Primault, J., Renou, S., Hublin, J.-J., Soressi, M., 2014. Les pratiques ornementales à l'Aurignacien ancien dans le Centre-Ouest de la France : l'apport des fouilles récentes aux Cottés (Vienne). Bulletin de la Société préhistorique française 111 (1), 21–40.

Roebroeks, W., Sier, M.J., Nielsen, T.K., De Loecker, D., Parés, J.M., Arps, C.E.S., Mücher, H.J., 2012. Use of red ochre by early Neandertals. ProcNatlAcadSci USA 109, 1889.

Rolland, N., Dibble, H.L., 1990. A new synthesis of middle Paleolithic variability. Am. Antiq. 55, 480–499.

Rudner, I.E., 1982. Khoisan Pigments and Paints and their Relationship to Rock Paintings. South African Museum, Cape Town.

Sacket, J.R., 1982. Approaches to style in lithic archaeology. J. Anthropol. Archaeol. 1, 59–112.

Sackett, J.R., 1986. Isochrestism and style: a clarification. J. Anthropol. Archaeol. 5, 266–277.

Salomon, H., 2009. Les matières colorantes au début du Paléolithique supérieur: sources, transformations et fonctions. Université Bordeaux 1, Bordeaux.

Shaham, D., Grosman, L., Goren-Inbar, N., 2010. The red-stained flint crescent from Gesher: new insights into PPNA hafting technology. J. Archaeol. Sci. 37, 2010–2016.

Soressi, M., d'Errico, F., 2007. Pigments, gravures, parures: les comportements symboliques controversés des Néandertaliens. In: Les Néandertaliens, Biologie et Cultures, Documents Préhistoriques. Vandermeersch, Bernard, Maureille, Bruno, Paris.

Turq, A., 2000a. Le paléolithique inférieur et moyen entre Dordogne et Lot, Paléo: Supplément. Société des amis du Musée national de Préhistoire et de la recherche archéologique.

Turq, A., 2000b. Les bases stratigraphiques régionales. Paléo, Revue d'Archéologie Préhistorique 45–74.

Turq, A., Dibble, H.L., Goldberg, P., McPherron, S.P., Sandgathe, D., Jones, H., Maddison, K., Maureille, B., Mentzer, S., Rink, J., Steenhuyse, A., 2011. Les Fouilles Récentes du Pech de l'Azé IV (Dordogne). Gallia Préhistoire 53, 1–58.

Turq, A., Roebroeks, W., Bourguignon, L., Faivre, J.-P., 2013. The fragmented character of Middle Palaeolithic stone tool technology. J. Hum. Evol. 65 (5), 641–655.

Vaquero, M., 2011. New perspectives on recycling of lithic resources using refitting and spatial data. Quartâr 58, 113–130.

Verna, C., d'Errico, F., 2011. The earliest evidence for the use of human bone as a tool. J. Hum. Evol. 60 (2), 145–157.

Wadley, L., Williamson, B., Lombard, M., 2004. Ochre in hafting in Middle Stone Age southern Africa: a practical role. Antiquity 78, 661–675.

Wadley, L., Hodgskiss, T., Grant, M., 2009. Implications for complex cognition from the hafting of tools with compound adhesives in the Middle Stone Age, South Africa. ProcNatlAcadSci USA 106, 9590.

Watts, I., 2002. Ochre in the middle stone age of Southern Africa: ritualised display or hide preservative? The South African Archaeological Bulletin 57 (175), 1–14.

Watts, I., 2009. Red ochre, body painting, and language: interpreting the blombos ochre. In: Botha, R., Knight, C. (Eds.), The Cradle of Language. Oxford University Press, Oxford, pp. 62–92.

Watts, I., 2010. The pigments from Pinnacle Point cave 13B, Western Cape, South Africa. J. Hum. Evol. 59 (3–4), 392–411.

Zilhão, J., Angelucci, D.E., Badal-García, E., d'Errico, F., Daniel, F., Dayet, L., Douka, K., Higham, T.F.G., Martínez-Sánchez, M.J., Montes-Bernárdez, R., Murcia-Mascarós, S., Pérez-Sirvent, C., Roldán-García, C., Vanhaeren, M., Villaverde, V., Wood, R., Zapata, J., 2010. Symbolic use of marine shells and mineral pigments by Iberian Neandertals.
ProcNatlAcadSci USA 107, 1023.

Archaeological information				Macroscopic examination						
N°	Layer	LTC*	Lithic typology	Colour	Length (cr	Width (cm	Thick. (cm)	Mass (g)	Type of blank	Type of oxide
CG-16	K (22)	Quina	Scrapers	Black	5.3	4.3	2.2	95.7	Raw nodule	Mn oxides
CG-17	K (22)	Quina	Scrapers	Gray/anthracite	2.3	2.0	1.4	8	Fragment	Mn oxides
CG-18	N (25)	Quina	Scrapers	Anthracite	3.6	2.2	1.1	11.8	Fragment	Mn oxides
CG-19	N (25)	Quina	Scrapers	Anthracite	3.3	1.8	0.9	6.3	Fragment	Mn oxides
CG-20	N (25)	Quina	Scrapers	Gray	2.2	2.0	0.7	4.1	Fragment	Mn oxides
CG-21	N (25)	Quina	Scrapers	Black/anthracite	6.5	22	21.9	13.8	Fragment	Mn-Co oxides
CG-22	N (25)	Quina	Scrapers	Black/anthracite	2	0.7	0.8	0.8	Worked fragment	Mn oxides
CG-23	N (25)	Quina	Scrapers	Black/anthracite	2	1.5	1.4	5.2	Worked fragment	Mn oxides
CG-24	N1 (26)	Quina	Scrapers	Gray	4.5	2.0	1.3	18.5	Worked nodule	Mn oxides
CG-25	M (24)	Quina	Scrapers	Anthracite	1.8	1.3	1.0	4	Worked fragment	Mn oxides
CG-26	N (25)	Quina	Scrapers	Gray	2.1	2.0	1.5	8	Worked fragment	Mn oxides
CG-27	N (25)	Quina	Scrapers	Gray	3.2	2.1	1.2	10.4	Worked fragment	Mn oxides
CG-28	M (24)	Quina	Scrapers	Black/anthracite	3.1	2.1	1.2	9	Worked fragment	Mn oxides + Fe oxides
CG-29	M (24)	Quina	Scrapers	Anthracite/gray	3.1	1.3	0.8	3.5	Flake	Mn oxides
CG-30	M (24)	Quina	Scrapers	Black/gray	3	1.8	1.5	11.1	Worked fragment	Mn oxides
CG-31	M (24)	Quina	Scrapers	Black/anthracite	3	2.4	1.3	14.5	Worked fragment	Mn oxides
CG-32	M (24)	Quina	Scrapers	Black/anthracite	2.3	1.3	1.1	5.1	Fragment	Mn oxides
CG-33	L (23)	Quina	Scrapers	Black/anthracite	1.5	1.1	0.7	1.8	Fragment	Mn oxides
CG-34	L (23)	Quina	Scrapers	Black/anthracite	1.3	0.6	0.4	0.6	Fragment	Mn oxides
CG-35	L (23)	Quina	Scrapers	Black/anthracite	1.2	0.8	0.6	1	Fragment	Mn oxides
CG-36	L (23)	Quina	Scrapers	Anthracite/brown yellow	2.3	1.4	1.2	4.4	Worked fragment	Mn oxides + Fe oxides
CG-37	L (23)	Quina	Scrapers	Grey/brown yellow	2.1	1.5	1.1	3.7	Fragment	Mn oxides
CG-38	L (23)	Quina	Scrapers	Black/anthracite	2.4	2.0	1.1	7.2	Worked fragment	Mn oxides
CG-39	L (23)	Quina	Scrapers	Anthracite/gray	2.3	1.4	1.0	5.3	Worked fragment	Mn oxides
CG-40	L (23)	Quina	Scrapers	Anthracite/ dark green	4.4	3.9	0.8	17.9	Cortical flake	Mn oxides
CG-41	L (23)	Quina	Scrapers	Anthracite	2.7	1.7	1.0	8.7	Worked fragment	Mn oxides
CG-42	L (23)	Quina	Scrapers	Anthracite	2.1	1.6	0.8	3	Fragment	Mn oxides
CG-43	L (23)	Quina	Scrapers	Anthracite	1.9	1.6	0.9	4	Worked fragment	Mn oxides
CG-44	L (23)	Quina	Scrapers	Anthracite gray	3.9	2.6	2.1	29.9	Worked fragment	Mn oxides
CG-45	L (23)	Quina	Scrapers	Anthracite gray	1.9	1.5	0.7	1.6	Fragment	Mn oxides
CG-46	L (23)	Quina	Scrapers	Anthracite gray	1.6	1.6	0.8	3.4	Fragment	Mn oxides
CG-47	L (23)	Quina	Scrapers	Anthracite gray	1.7	1.5	0.9	2.6	Fragment	Mn oxides
CG-48	L (23)	Quina	Scrapers	?	1.8	1.4	0.6	2.3	Worked fragment	Mn oxides
CG-49	L (23)	Quina	Scrapers	Anthracite	2	1.6	0.8	3.7	Fragment	Mn oxides
CG-50	L (23)	Quina	Scrapers	Gray/dark brown	2.2	2.0	1.9	10.5	Fragment	Mn oxides
CG-51	L (23)	Quina	Scrapers	Dark brown, dark red	3.3	2.5	1.1	12.2	Fragment	Fe oxides + Mn oxides
CG-52	L (23)	Quina	Scrapers	Black, dark red	2.3	1.8	0.8	6.2	Fragment	Fe oxides
CG-53	L (23)	Quina	Scrapers	White	2.2	1.8	0.6	2.1	?	Calcite, chalk
CG-54	L (23)	Quina	Scrapers	White	2.5	1.6	1.1	3.5	?	Calcite, chalk
CG-55	L (23)	Quina	Scrapers	White	1.6	1.5	0.8	2	?	Calcite, chalk
CG-56	K (22)	Quina	Scrapers	Anthracite/gray	1.3	1.2	1.0	3	Worked fragment	Mn oxides
CG-57	K (22)	Quina	Scrapers	Black	2.5	2.2	1.5	9.6	Worked fragment	Mn oxides
CG-58	K (22)	Quina	Scrapers	Black	2.4	2.1	0.7	7.9	Worked fragment	Mn oxides
CG-59	K1 (21)	Quina	Scrapers	Gray	1.8	1.1	0.6	2	Worked fragment	Mn oxides
CG-60	K (22)	Quina	Scrapers	Ocre, rouge, jaune	8.2	7.7	5.6	400.1	?	Fe oxides
CG-61	J (18)	Quina	Denticulates/scrapers	Antracite/brown	3.4	4.0	2.7	61.3	Worked fragment	Mn oxides
CG-62	I (17)	Quina	Denticulates/scrapers	Dark red purple, ligtht brown	1.5	1.3	0.4	1.3	?	Fe oxides
CG-63	I (17)	Quina	Denticulates/scrapers	Antrhacite/gray	1.5	1.3	0.8	2.8	?	Mn oxides
CG-64	I (17)	Quina	Denticulates/scrapers	Dark red	5.2	4.1	0.8	25.1	Raw nodule	Fe oxides
CG-65	I (17)	Quina	Denticulates/scrapers	Yellow, brown	2.9	1.6	0.7	2.5	?	Fe oxides
CG-66	H2 (16)	Lev./Disc. Bladelet	Denticulates	Anthracite/gray	4.3	3.7	2.0	50.7	Fragment	Mn oxides
CG-67	H (15)	Discoid	Denticulates	Anthracite/brown yellow	2	1.3	0.8	3.2	?	Mn oxides
CG-68	H (15)	Discoid	Denticulates	Dark red/ dark yellow	3.8	3.3	3.1	53.4	Fragment	Fe oxides
CG-69	H (15)	Discoid	Denticulates	Dark red/ dark yellow	2.6	2.1	1.3	6.7	Fragment	Fe oxides
CG-70	H (15)	Discoid	Denticulates	Dark red/ black/dark yellow	1.8	1.8	0.9	3.2	Fragment	Fe oxides
CG-71	H (15)	Discoid	Denticulates	Dark red/ dark yellow	1.7	1.2	0.4	0.9	?	Fe oxides
CG-72	H (15)	Discoid	Denticulates	Dark red/ dark yellow	2.1	1.3	1.2	3.5	Fragment	Fe oxides
CG-73	H (15)	Discoid	Denticulates	Dark red/ black/dark yellow	1.8	1.2	0.6	1.4	Flake?	Fe oxides
CG-74	H (15)	Discoid	Denticulates	White	2.7	1.2	0.8	3.1	?	Calcite, chalk
CG-75	G (14)	Discoid	Denticulates	Dark red/ black/dark yellow	6	5.3	3.6	91.6	Fragment	Fe oxides
CG-76	G (14)	Discoid	Denticulates	Dark red/ black	3.5	3.2	2.2	19.2	Fragment	Fe oxides
CG-77	G (14)	Discoid	Denticulates	Dark red/black	2.8	2.3	1.3	8.9	Fragment	Fe oxides
CG-78	G (14)	Discoid	Denticulates	Dark red/ red	4.7	3.0	1.8	12.9	Flake/fragment	Fe oxides
CG-79	G (14)	Discoid	Denticulates	Red	2.9	1.5	1.3	6.6	Fragment	Fe oxides
CG-80	G (14)	Discoid	Denticulates	Red	3.2	1.4	0.9	3.9	Fragment	Fe oxides
CG-81	G (14)	Discoid	Denticulates	Light pink, dark red	2.1	2.2	1.4	6.3	?	Fe oxides
CG-82	E2 (12)	Discoid/Levallois	Denticulates	Dark red/ black/dark yellow	7.5	5.4	4.3	169.9	Fragment	Fe oxides
CG-83	E2 (12)	Discoid/Levallois	Denticulates	Dark red/ dark yellow	3	3.0	2.2	19.5	Fragment	Fe oxides
CG-84	E2 (12)	Discoid/Levallois	Denticulates	Light brown, anthracite/dark brow	4.2	2.9	2.6	28.6	?	Fe oxides
CG-85	E2 (12)	Discoid/Levallois	Denticulates	Light pink, dark red	2.4	1.7	1.6	6.3	?	Fe oxides
CG-86	E1 (11)	Discoid/Levallois	Denticulates	Anthracite/dark brown	3.5	2.0	1.6	17.8	Fragment	Mn oxides
CG-87	E1 (11)	Discoid/Levallois	Denticulates	Dark red/black	2.8	2.6	1.6	17.7	Fragment	Fe oxides
CG-88	E1 (11)	Discoid/Levallois	Denticulates	Light pink, dark red	1.7	1.3	1.3	3	Fragment	Fe oxides

*Lithic technocomplexe

Outcrop co	Town	Lieu-dit'	Location of the occurrences	Latitude	Longitude	Geological description	Formation
D1	Domme	Jacoumard	Astragale along a road	N44°48'10''	E1°15'15.5''	Concretions within alteritic sands	Alterites
D2		Jacoumard	Astragale along a road	N44°48'26''	E1°15'04''	Concretions and nodules within brown soil	Alterites
D3		Liaubou bas	Sand quarry	N44°47'02.5''	E1°17'31.5''	Concretions and veins within alteritic sands	Alterites
D4		Combe-Grenal	Section along a road	N44°48'23''	E1°13'34.5''	Veins within fresch limestone	Coniacian
D5		Giverzac	Covering the soil	N44°48'38''	E1°14'42''	Nodules within a brown soil	Pedogenic
D6		Combe-Grenal	Astragale along a stream	N44°48'22''	E1°13'48''	Nodules within a brown soil	Pedogenic
D7		Combe-Grenal	Astagale along a stream	N44°48'22''	E1°13'29.5''	Nodules within a brown soil	Pedogenic
C1	La Canéda	Curboursil	Covering the soil	N44°51'02''	E1°13'41''	Nodules within a brown soil	Pedogenic
Huy	Huy (Belgium)		Section along a road			Oolithic hematite	Lower Famenian

		Petrology		Elemental composition SEM		Mineralogy DRX	
Layer		Rock texture	Rock fabric	Mn / Fe phases*	Other phases*	Mn or Fe phases	Other minerals
Manganese oxides							
CG17	**22**	Clay-sand	Massive, crystalline	**Mn**-(Si) + **Mn**-Ba	Si, Al, K (Fe)	-	-
CG21	**25**	Clay-silt	Granular	**Mn**-Al-(Co)	Al, Si, Fe, K	Lithiophorite (manganosite)	**Quartz** (bohmite?)
CG23	**25**	Sand	Massive	**Mn**-(Fe, Al, Si)	Si, Al	**-**	-
CG26	**25**	Clay-sand	Massive, crystalline	**Mn** + **Mn**-Ba	Si	**Pyrolusite** (Ramsdellite?)	(Quartz)
CG27	**25**	Clay-sand	Massive, crystalline	**Mn**-Ba + **Mn**	(Al)	**Pyrolusite** (Ramsdellite?)	-
CG28	**24**	Clay-silt	Granular	**Mn**-Fe-(Si, Al) + **Fe**-Mn-(Si, Al)	Si	**Pyrolusite,** Goethite, manganite (Birnessite/kaolinite group)	Quartz
CG30	**24**	Sand	Massive	**Mn**-(Fe, Al, Si)	Si	**-**	-
CG31	**24**	Sand	Massive	**Mn**-(Si, Al, Fe, Ba)	Si, Al, Fe	**Pyrolusite,** Ramsdellite, Birnessite/koalinite group	(Quartz?)
CG36	**23**	Sand	Massive	**Mn**-Fe		**Pyrolusite**, Goethite	(Quartz)
CG40	**23**	Clay-silt	Granular	**Mn**-(Fe)	Si, Al	**-**	-
CG41	**23**	Sand	Massive	**Mn** + **Mn**-Ba	Si, Al (Fe, K, Ba)	**Pyrolusite**	(Quartz)
CG47	**23**	Clay-silt	Finely granular	Mn-Si-Al-(Ba, Fe) + **Mn**-Ba + **Mn**-Fe	Si, Fe, Al	**-**	-
CG48	**23**	Sand	Massive	**Mn**-Ba-(Si, Al)	Si, Al, Fe (Mg, Ti)	**-**	-
CG49	**23**	Sand	Massive, granular cortex	**Mn +** Mn-Mg-Si	Si, Al (Fe, Ca, K)	**Pyrolusite**	(Quartz)
CG58	**22**	Sand	Lightly laminated	**Mn**-(Si)	Ca, P, Si (Al)	Pyrolusite, Manganite (Birnessite/kaolinite group)	**Quartz, h**ydroxylapatite
CG59	**21**	Clay-sand	Massive, crystalline	**Mn**	Si, Al, Ca, Fe, (P, K)	**-**	-
CG67	**15**	Sand	Massive	**Mn**	Ca, Si, Al (Fe, K)	**-**	-
CG84	**12**	Clay-sand	Massive, mixed	**Mn**-Ba	Ca, Si, Al (Fe)	**-**	-
CG86	**11**	Clay-sand	Granular, massive	**Mn**	Ca, Si, Al (P, K)	Pyrolusite (manganite?)	**Calcite,** quartz
Iron oxides							
CG52	**23**	Clay-silt	Botryoïdal	**Fe**-(Si, Al)	Si,Al (K)	**Goethite**	Quartz, calcite
CG65	**17**	Sand	Lightly laminated	**Fe**-(Si, Al)	Ca, Si, Al, Fe (K)	Goethite	**Calcite,** quartz (clay mineral?)
CG69	**15**	Clay-silt	Granular	**Fe**-Si-(Al)	Si, Al, Fe, Ca (K, Mn)	**Goethite**	Quartz
CG70	**15**	Sand	Massive, concentric lamination	**Fe**-(Si, Al)	Si, Al, Fe, Ca	-	-
CG76	**14**	Sand	Massive	**Fe**-(Si, Al)	Si, Al, Fe, Ca (P)	**-**	-
CG77	**14**	Clay-silt	Granular, laminated	**Fe**-(Si, Al)	Si, Fe, Al (K, Ca)	**Hematite**	Quartz
CG78	**14**	Clay-silt	Granular	**Fe**-Si-(Al)	Si (Fe, Al)	-	-
CG79	**14**	Clay-silt	Massive	**Fe**-(Si, Al)	Si, Ca, Fe (Al, K)	**Hematite, Goethite**	Quartz, calcite
CG81	**14**	Clay-sand	Massive, granular	**Fe**-(Si, Al) + **Fe**-Mn	Si, Al, Fe	**-**	-
CG83	**12**	Clay-sand	Massive, concentric lamination	**Fe**-(Si, Al) + Fe-(Mn)	Si, Al, Fe (K, Ti)	-	-
CG85	**12**	Clay-sand	Massive, granular	**Fe**-Si-(Al)	Ca, Si, Al (K)	**-**	-
CG87	**11**	Sand	Massive	**Fe**-(Si, Al)	Si, Ca (Al, K)	**Goethite**	Quartz (chlorite? Calcite?)
White piece							
CG74	**15**	Clay	Massive	Ca		**-**	-

*In brakets: minor element
In bold: main element

	No traces	%	Possible striations	%	Grinding	%	Grinding/s craping	%	scraping	%	Total
Mn oxides*	15	*34.9*	2	*4.7*	6	*14.0*	2	*4.7*	18	*41.9*	43
Fe oxides*	25	*100.0*	0	*0.0*	0	*0.0*	0	*0.0*	0	*0.0*	25
Calcite, chalk	4	*100.0*	0	*0.0*	0	*0.0*	0	*0.0*	0	*0.0*	4
Total	44	*61.1*	2	*2.8*	6	*8.3*	2	*2.8*	18	*25.0*	72

**Major component*

	Layers/Levels	Bordes' facies	LTC after revision (Flaking system)	Typology after revision	Mineral pigments Nature	References
Charente						
La Quina	Moustérien supérieur'	MTA	?	?	Mostly Mn oxide	Martin 1923
Corrèze						
La-Chapelle-aux-Saints	?	Quina	?	?	Fe oxide	Demars 1992
Dordogne						
Combe Grenal	12-16	Denticulates	Discoid, Discoid/levallois	Denticulates	Mostly Fe oxide	Demars 1992; Faivre et al. 2014; This study
	26-17	Quina		Scrapers and denticulates	Mostly Mn oxide	Demars 1992; Faivre et al. 2014; This study
Le Moustier	H	MTA	Discoid	Denticulates	Mostly Mn oxide	Demars 1992; Gravina and Discamps 2015
	G3-G4	MTA	Bifacial	Bifacial pieces	Mostly Mn oxide	Demars 1992; Gravina 2017
	G1-G2	MTA	Levallois	Bifacial pieces	Mostly Mn oxide	Demars 1992; Gravina 2017
Pech de l'Azé I	4	MTA	Bifacial	Bifacial pieces	Mostly Mn oxide	Demars 1992; Soressi and d'Errico 2007
Pech de l'Azé IV	F	MTA	Discoid	?	Mostly Mn oxide	Demars 1992
	I-J	Typical Mousterian	Levallois?	?	Mostly Mn oxide	Demars 1992
Caminade	3b-2	La Ferrassie Mousterian	Levallois?	?	Mostly Mn oxide	de Sonneville-Bordes 1969; Demars 1992